

Article

Potential Surviving Effect of *Cleome droserifolia* Extract against Systemic *Staphylococcus aureus* Infection: Investigation of the Chemical Content of the Plant

Jawaher Alqahtani ^{1,*}, Walaa A. Negm ², Engy Elekhawy ^{3,*}, Ismail A. Hussein ⁴, Hassan Samy Hassan ⁵, Abdullah R. Alanzi ¹, Ehssan Moglad ⁶, Rehab Ahmed ⁷, Sarah Ibrahim ⁸ and Suzy A. El-Sherbeni ²

¹ Department of Pharmacognosy, College of Pharmacy, King Saud University, Riyadh 11495, Saudi Arabia; aralonazi@ksu.edu.sa

² Department of Pharmacognosy, Faculty of Pharmacy, Tanta University, Tanta 31527, Egypt; walaa.negm@pharm.tanta.edu.eg (W.A.N.); suzy.elsherbini@pharm.tanta.edu.eg (S.A.E.-S.)

³ Department of Pharmaceutical Microbiology, Faculty of Pharmacy, Tanta University, Tanta 31527, Egypt

⁴ Department of Pharmacognosy and Medicinal Plants, Faculty of Pharmacy (Boys), Al-Azhar University, Cairo 11884, Egypt; ismaila.hussein@azhar.edu.eg

⁵ Faculty of Pharmacy, Tanta University, Tanta 31527, Egypt; hasan30998367@pharm.tanta.edu.eg

⁶ Department of Pharmaceutics, College of Pharmacy, Prince Sattam bin Abdulaziz University, P.O. Box 173, Alkharj 11942, Saudi Arabia; e.moglad@psau.edu.sa

⁷ Department of Natural Products and Alternative Medicine, Faculty of Pharmacy, University of Tabuk, Tabuk 47713, Saudi Arabia; rahmed@ut.edu.sa

⁸ Human Anatomy and Embryology Department, Faculty of Medicine, Tanta University, Tanta 31527, Egypt; sara.ibrahim@med.tanta.edu.eg

* Correspondence: jalqahtani@ksu.edu.sa (J.A.); engy.ali@pharm.tanta.edu.eg (E.E.)



Citation: Alqahtani, J.; Negm, W.A.; Elekhawy, E.; Hussein, I.A.; Hassan, H.S.; Alanzi, A.R.; Moglad, E.; Ahmed, R.; Ibrahim, S.; El-Sherbeni, S.A.

Potential Surviving Effect of *Cleome droserifolia* Extract against Systemic *Staphylococcus aureus* Infection: Investigation of the Chemical Content of the Plant. *Antibiotics* **2024**, *13*, 450. <https://doi.org/10.3390/antibiotics13050450>

Academic Editors: Eliana De Gregorio and Anna Esposito

Received: 21 April 2024

Revised: 13 May 2024

Accepted: 13 May 2024

Published: 15 May 2024



Copyright: © 2024 by the authors. Licensee MDPI, Basel, Switzerland. This article is an open access article distributed under the terms and conditions of the Creative Commons Attribution (CC BY) license (<https://creativecommons.org/licenses/by/4.0/>).

Abstract: The increasing rates of morbidity and mortality owing to bacterial infections, particularly *Staphylococcus aureus* have necessitated finding solutions to face this issue. Thus, we elucidated the phytochemical constituents and antibacterial potential of *Cleome droserifolia* extract (CDE). Using LC-ESI-MS/MS, the main phytoconstituents of CDE were explored, which were kaempferol-3,7-O-bis-alpha-L-rhamnoside, isorhamnetin, cyanidin-3-glucoside, kaempferide, kaempferol-3-O-alpha-L-rhamnoside, caffeic acid, isoquercitrin, quinic acid, isocitrate, mannitol, apigenin, acacetin, and naringenin. The CDE exerted an antibacterial action on *S. aureus* isolates with minimum inhibitory concentrations ranging from 128 to 512 µg/mL. Also, CDE exhibited antibiofilm action using a crystal violet assay. A scanning electron microscope was employed to illuminate the effect of CDE on biofilm formation, and it considerably diminished *S. aureus* cell number in the biofilm. Moreover, qRT-PCR was performed to study the effect of CDE on biofilm gene expression (*cna*, *fnbA*, and *icaA*). The CDE revealed a downregulating effect on the studied biofilm genes in 43.48% of *S. aureus* isolates. Regarding the *in vivo* model, CDE significantly decreased the *S. aureus* burden in the liver and spleen of CDE-treated mice. Also, it significantly improved the mice's survival and substantially decreased the inflammatory markers (interleukin one beta and interleukin six) in the studied tissues. Furthermore, CDE has improved the histology and tumor necrosis factor alpha immunohistochemistry in the liver and spleen of the CDE-treated group. Thus, CDE could be considered a promising candidate for future antimicrobial drug discovery studies.

Keywords: antibiotic resistance; biofilm; systemic infection; LC-ESI-MS/MS; qRT-PCR; inflammatory markers

1. Introduction

Cleome droserifolia (Forssk.) Delile Descr. is a small shrub that can grow to 60 cm in height. It grows naturally in Egyptian deserts like the Sinai Peninsula, stone soil, and rocky wadis. It became endangered due to extensive uprooting in Egypt's Sinai and Eastern

Deserts [1,2]. The genus *Cleome* (L.) DC. (Cleomaceae) [3] encompasses annual and perennial medicinal herbs or small shrubs [4–7]. *Cleome droserifolia*, known by local Bedouin people as Samwah, is employed in traditional medicine in Egypt as a hypoglycemic agent [8,9]. Different researchers analyzed the phytochemical content of *C. droserifolia*, exploring the existence of flavonoids [10], alkaloids, tannins, saponins, coumarins, catechins, sterols, glucosinolates, and terpenoids [1,9]. The essential oil profile of *C. droserifolia* was also studied, and the main compounds in the essential oil were (*Z*)-nerolidol and α -cadinol [11]. *C. droserifolia* exerted different biological effects as an antioxidant, antimicrobial [12], anticancer [13], allelopathic [11], and hypoglycaemic [14] properties.

Staphylococcus aureus is a common species of *Staphylococci* highly associated with multidrug resistance [15]. Such bacterial species can adapt to various environments and possess frequent virulence factors [16]. In addition, it is a common nosocomial pathogen that can trigger various diseases that range from mild severity to life-threatening ailments. The infections triggered by *S. aureus* are mild skin and soft tissue infections, bacteremia, osteomyelitis, endocarditis, and pneumonia [17].

S. aureus can exhibit resistance to antibiotics by various mechanisms, including decreasing the bacterial membrane permeability to the antibiotics, efflux, and excessive production of resistance enzymes like β -lactamases [18]. Multi-drug resistance (MDR) is a worldwide issue that has a deleterious effect on health care. *S. aureus* acquires resistance to antibiotics owing to persistent exposure to various antimicrobials. MDR *S. aureus* is resistant to multiple chemotherapeutic agents. Such MDR isolates have led to increasing global rates of mortality as well as morbidity in *S. aureus*-infected patients [19].

Biofilm is an important virulence factor of *S. aureus*, and it is defined as an extracellular complex structure that compromises a population of bacterial cells anchored to living or non-living surfaces [20]. The cells are surrounded by an extracellular polymer matrix formed by themselves as a protective tactic for bacterial survival to adapt to their surrounding environments [21].

Traditional antibiotics are excessively losing their potential to combat bacterial infections, particularly *S. aureus* [22]. Thus, novel treatment approaches should be elucidated to face such global concerns. Natural sources, like plants, are rich in many bioactive phytochemicals with various therapeutic activities [23]. Many studies have elucidated the potential antimicrobial action of plants and their bioactive constituents against viruses, fungi, and bacteria [24–28].

Here, we aimed to explore CDE's potential antibacterial action *in vitro* and *in vivo*. Also, the phytoconstituents of this plant will be elucidated using liquid chromatography-electrospray ionization-tandem mass spectrometry (LC-ESI-MS/MS) to explore the active principles with different chemical entities which may have a role in developing new antibacterial agents against the MDR *S. aureus* isolates.

2. Results

2.1. Recognition of Different Phytochemical Contents of *C. droserifolia* by LC-ESI-MS/MS

It was revealed tentatively by this technique that *C. droserifolia* contains different phytochemical groups with variable biological effects. This plant contains dicarboxylic and tricarboxylic acids and their derivatives, hydroxy fatty acids, hydroxybenzoic acid derivatives, flavonols, flavones, flavanones, aurone O-glycosides, hydroxycinnamic acids, quinic acids and derivatives, flavonoid-3-O-glycosides, anthocyanidin-3-O-glycosides, anthocyanidin-5-O-glycosides, alkyl glucosinolate, methoxy phenols, and 4'-O-methylated flavonoids. The LC-ESI-MS/MS analysis disclosed that the predominant constituents are kaempferol-3,7-O-bis- α -L-rhamnoside, isorhamnetin, cyanidin-3-glucoside, 3, 5, 7-trihydroxy-4'-methoxyflavone (kaempferide), kaempferol-3-O- α -L-rhamnoside, caffeic acid, isoquercitrin, quinic acid, isocitrate, mannitol, apigenin, acacetin, and naringenin. Table 1 and Figure S1 in the Supplementary Materials demonstrate the tentatively recognized compounds supported by referenced data. The previously reported data revealed the presence of different phenolic compounds in *C. droserifolia*, such as

kaempferol-3,7-dirhamnoside, isorhamnetin-3-O-gluco-7-O-rhamnoside, kaempferol-3-O-gluco-7-O-rhamnoside, quercetin-3-O-gluco-7-O-rhamnoside, kaempferol, artemitin [9], Isorhamnetin-3-O- β -D-glucoside, quercetin-3'-methoxy-3-O-(4''-acetyl rhamnoside)-7-O- α -rhamnoside, and kaempferol-4'-methoxy-3,7-dirhamnoside [29]. It was detected by RP-HPLC of the methanolic extract of the plant that the major phenolic compounds were benzoic acid, ellagic acid, rutin, o-coumaric acid, and naringenin. Moderate quantities of rosmarinic acid, p-hydroxybenzoic acid, resveratrol, kaempferol, quercetin, and ferulic acid were detected. The least abundant phenolic compounds were chlorogenic acid, caffeic acid, p-coumaric acid, syringic acid, and catechin [12].

Table 1. The phytoconstituents of *C. droserifolia* methanol extract recognized by LC-ESI-MS/MS analysis.

	RT (min)	Compound Name	Precursor m/z	Error ppm	Formula	MS/MS	Ontology	Reference
1	0.821	Succinic acid	117.0192 [M – H] [−]	−0.2	C ₄ H ₆ O ₄	73.21, 100.00, 117.07	Dicarboxylic acids and derivatives	[30]
2	0.821	3-Hydroxy-3-Methylglutaric acid (Meglutol)	161.0471 [M – H] [−]	−7.8	C ₆ H ₁₀ O ₅	56.85, 113.05, 131.03, 143.04, 161.02	Hydroxy fatty acids	[31]
3	0.860	cis-Aconitate	173.0816 [M – H] [−]	0.4	C ₆ H ₆ O ₆	111.43, 129.12, 173.02	Tricarboxylic acids derivatives	[32]
4	0.912	D-(-)-Quinic acid	191.0553 [M – H] [−]	3.2	C ₇ H ₁₂ O ₆	111.02, 155.02, 164.02, 173.02, 191.77	Quinic acids and derivatives	[33]
5	0.939	Catechol	109.0291 [M – H] [−]	0.8	C ₆ H ₆ O ₂	53.03, 65.00, 81.03, 91.02, 109.02	Catechols	[34]
6	0.940	3,4-dihydroxy benzoic acid	153.0191 [M – H] [−]	0.1	C ₇ H ₆ O ₄	53.03, 79.95, 108.12, 153.01	Hydroxybenzoic acid derivatives	[35]
7	9.581	3, 5, 7-trihydroxy-4'-methoxyflavone (kaempferide)	299.0563 [M – H] [−]	0.2	C ₁₆ H ₁₂ O ₆	64.02, 107.00, 151.09, 164.12, 253.63, 284.53, 299.01	Flavonols	[36]
8	1.006	Maleic acid	115.0388 [M – H] [−]	7.4	C ₄ H ₄ O ₄	69.03, 71.04, 115.04	Dicarboxylic acids and derivatives	[37]
9	1.256	Isorhamnetin	315.0754 [M – H] [−]	−8.9	C ₁₆ H ₁₂ O ₇	56.01, 135.02, 109.03, 151.04, 163.04, 255.42, 271.12, 300.23, 315.16	Flavonol	[38]
10	1.138	Mannitol	181.0728 [M – H] [−]	−4.4	C ₆ H ₁₄ O ₆	59.02, 71.32, 89. 14, 101.05, 163.05, 181.99	Sugar alcohols	[39]
11	1.152	Caffeic acid	179.0567 [M – H] [−]	−2.2	C ₉ H ₈ O ₄	77.70, 89.03, 117.10, 134.09, 161.05, 179.06	Hydroxycinnamic acids	[40]
12	3.321	p-Coumaric acid	163.0401 [M – H] [−]	−0.7	C ₉ H ₈ O ₃	65.97, 91.03, 107.03, 119.04, 163.04	Hydroxycinnamic acids	[41]

Table 1. Cont.

	RT (min)	Compound Name	Precursor <i>m/z</i>	Error ppm	Formula	MS/MS	Ontology	Reference
13	3.346	(R)-2-hydroxy-3-butenyl glucosinolate	388.0759 [M – H] [–]	–3.4	C ₁₁ H ₁₉ NO ₁₀ S ₂	195.02, 241.14, 259.00, 290.97, 388.03	Alkyl glucosinolates	[42]
14	4.432	Esculin	339.0709 [M – H] [–]	0.4	C ₁₅ H ₁₆ O ₉	69.01, 121.09, 178.84, 320.10, 339.34	Coumarin glycosides NIST	[43]
15	5.318	Chlorogenic acid	353.0841 [M – H] [–]	7.2	C ₁₆ H ₁₈ O ₉	135.02, 161.02, 179.11, 191.06, 353.20	Quinic acids and derivatives	[44]
16	5.460	Isoquercitrin	463.0854 257; 229; 201; 150; 155	4.6	C ₂₁ H ₂₀ O ₁₂	65.00, 150.99, 229.95, 257.04, 463.04	Flavonoid-3-O-glycosides	[45]
17	5.5115	Luteolin	285.1688 [M – H] [–]	4.4	C ₁₅ H ₁₀ O ₆	216.98, 199.04, 175.04, 151.01, 285.03	Flavones	[46]
18	5.798	Kaempferol-3-O-(6-p-coumaroyl)-glucoside	593.1558 [M – H] [–]	–6.5	C ₃₀ H ₂₆ O ₁₃	56.04, 447.11, 430.91, 307.21, 285.18	Flavonoid 3-O-p-coumaroyl glycosides	[46]
19	5.987	Syringetin-3-O-glucoside	507.1159 [M – H] [–]	–2.2	C ₂₃ H ₂₄ O ₁₃	112.98, 302.89, 329.94, 345.08, 507.01	Flavonoid-3-O-glycosides	[47]
20	6.101	Delphinidin-3-O-β-glucopyranoside (Myrtillin A)	463.0253 [M – 2H] [–]	–1.7	C ₂₁ H ₂₁ O ₁₂	125.02, 271.018, 300.05, 301.02, 463.03	Anthocyanidin-3-O-glycosides	[48]
21	6.254	Cyanidin-3-glucoside	447.0908 [M – H] [–]	4.4	C ₂₁ H ₂₁ O ₁₁	147.05, 227.00, 256.20, 285.42, 447.07	Anthocyanidin-3-O-glycosides	[48,49]
22	6.329	Luteolin-3',7-di-O-glucoside	609.1434 [M – H] [–]	3.2	C ₂₇ H ₃₀ O ₁₆	112.97, 253.00, 285.14, 399.05, 447.144, 489.02, 609.13	Flavonoid-7-O-glycosides	[50]
23	6.374	3-(4-hydroxy-3,5-dimethoxyphenol)-2-propenoic acid sinapic acid or sinapinic acid	223.0618 [M – H] [–]	–2	C ₁₁ H ₁₂ O ₅	59.01, 175.03, 207.04, 223.13	Hydroxycinnamic acids	[51]
24	6.601	Quercitrin	447.1836 [M – H] [–]	3.9	C ₂₁ H ₂₀ O ₁₁	152.11, 300.18, 301.12, 447.12	Flavonoid-3-O-glycosides	[52]
25		quercetin-3'-methoxy-3O-(4''-acetyl)rhannoside)-7-O-rhannoside	665.165 [M – H] [–]		C ₃₀ H ₅₀ O ₁₆	315.16, 461.01, 519.32, 665.21	Flavonoid-3-O-glycosides	[53]
26	6.614	Isocitrate	191.0334 [M – H] [–]	4.3	C ₆ H ₈ O ₇	76.03, 107.01, 149.02, 191.02	Tricarboxylic acids and derivatives	[54]
27	6.764	Benzyl glucosinolate	407.0401 [M – H] [–]	–0.7	C ₁₄ H ₁₈ NO ₉ S ₂	212.03, 240.99, 259.00, 274.01, 328.07, 407.04	Hydroxy cinnamic acids	[42,55]

Table 1. Cont.

	RT (min)	Compound Name	Precursor <i>m/z</i>	Error ppm	Formula	MS/MS	Ontology	Reference
28	6.891	Kaempferol-3- <i>O</i> - α -L-rhamnoside	431.099 [M – H] [–]	–0.7	C ₂₁ H ₂₀ O ₁₀	89.05, 285.13, 313.12, 395.03, 430.96, 431.45	Flavonoid-3- <i>O</i> -glycosides	[56]
29	7.013	Isorhamnetin-3- <i>O</i> -rutinoside	623.163 [M – H] [–]	–1.1	C ₂₈ H ₃₂ O ₁₆	151.00, 165.01, 315.23, 623.72	Flavonoid-3- <i>O</i> -glycosides	[57]
30	7.025	Peonidin-3,5- <i>O</i> -di- β -glucopyranoside	623.0959 [M – 2H] [–]	–3	C ₂₈ H ₃₃ O ₁₆	59.01, 301.01, 463.11, 623.16	Anthocyanidin-5- <i>O</i> -glycosides	[58]
31	7.062	Delphinidin-3- <i>O</i> -(6''- <i>O</i> - α -rhamnopyranosyl-beta-glucopyranoside)	609.2933 [M – 2H] [–]	–7.1	C ₂₇ H ₃₁ O ₁₆	125.01, 300.03, 301.01, 447.16, 462.91, 609.13	Anthocyanidin-3- <i>O</i> -glycosides	[46,48]
32	7.515	Kaempferol-3,7- <i>O</i> -bis- α -L-rhamnoside	577.1559 [M – H] [–]	0.7	C ₂₇ H ₃₀ O ₁₄	285.0405, 431.0969, 577.43	Flavonoid-7- <i>O</i> -glycosides	[46]
33	7.552	Kaempferol-3- <i>O</i> - α -L-arabinoside	417.0826 [M – H] [–]	–1.9	C ₂₀ H ₁₈ O ₁₀	258.43, 285.32, 313.02, 417.33	Flavonoid-3- <i>O</i> -glycosides	[59]
34		kaempferol-4'-methoxy-3,7-dirhamnoside	591.24 [M – H] [–]		C ₂₈ H ₃₂ O ₁₄	285.02, 299.21, 445.02, 591.11	Flavonoid-3- <i>O</i> -glycosides	[60]
35		isorhamnetin-3- <i>O</i> - β -D-glucoside	477.23 [M – H] [–]			269.98, 300.52, 315.03, 477.03	Flavonoid-3- <i>O</i> -glycosides	[59,61]
36	7.564	Hesperetin	301.1482 174.92, 255.22, 301.06 [M – 2H] [–]	–2.9	C ₁₆ H ₁₄ O ₆	153.10, 177.61, 273.13, 273.06, 301.00	4'- <i>O</i> -methylated flavonoids	[62]
37	7.626	Apigenin	269.1399 [M – H] [–]	0.3	C ₁₅ H ₁₀ O ₅	149.01, 151.09, 183.12, 225.05, 241.00, 269.06	Flavones	[63]
38	7.851	Naringenin	271.0617 [M – H] [–]	0.7	C ₁₅ H ₁₂ O ₅	63.02, 151.00, 177. 227.08, 227.06, 271.06	Flavanones	[64]
39	8.009	apigenin-7- <i>O</i> -glucoside	431.0987 [M – H] [–]	–0.6	C ₂₁ H ₂₀ O ₁₀	268.14, 269.09, 310.88, 431.02	Flavonoid-7- <i>O</i> -glycosides	[65]
40	8.136	Peonidine-3- <i>O</i> -glucoside	461.1121 [M – 2H] [–]	–4.2	C ₂₂ H ₂₃ O ₁₁	71.01, 79.05, 89.02, 301.98, 461.30	Anthocyanidin-3- <i>O</i> -glycosides	[48,58]
41	8.274	Daidzein-8- <i>C</i> -glucoside	415.1986 [M – H] [–]	–1.2	C ₂₁ H ₂₀ O ₉	249.14, 267.03, 295.16, 325.20, 379.23, 415.87	Isoflavonoid C-glycosides	[66,67]
42	8.999	Syringaldehyde	181.051 [M – H] [–]	0.8	C ₉ H ₁₀ O ₄	99.97, 136.00, 151.02, 166.04 181.09	Methoxy phenols	[36]
43	10.301	Maritimetin-6- <i>O</i> -glucoside	447.2719 [M – H] [–]	1.8	C ₂₁ H ₂₀ O ₁₁	57.03, 132.71, 151.03, 285.05, 447.32	Aurone O-glycosides	[46]
44	13.88	Acacetin	283.0594 [M – H] [–]	5.1	C ₁₆ H ₁₂ O ₅	151.08, 252.13, 240.04, 268.03, 283.26	4'- <i>O</i> -methylated flavonoids	[63,68]

2.2. Bacterial Isolates and Antibiotic Resistance

The clinical specimens from which the bacterial isolates were recovered include blood, wounds, sputum, and urine (Figure 1). The antibiotic susceptibility of the tested isolates is revealed in Figure 2.

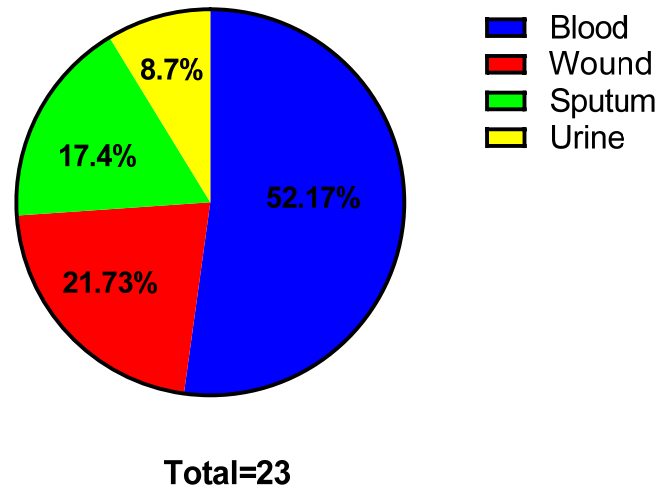


Figure 1. Pie chart revealing the percentages of the clinical specimens.

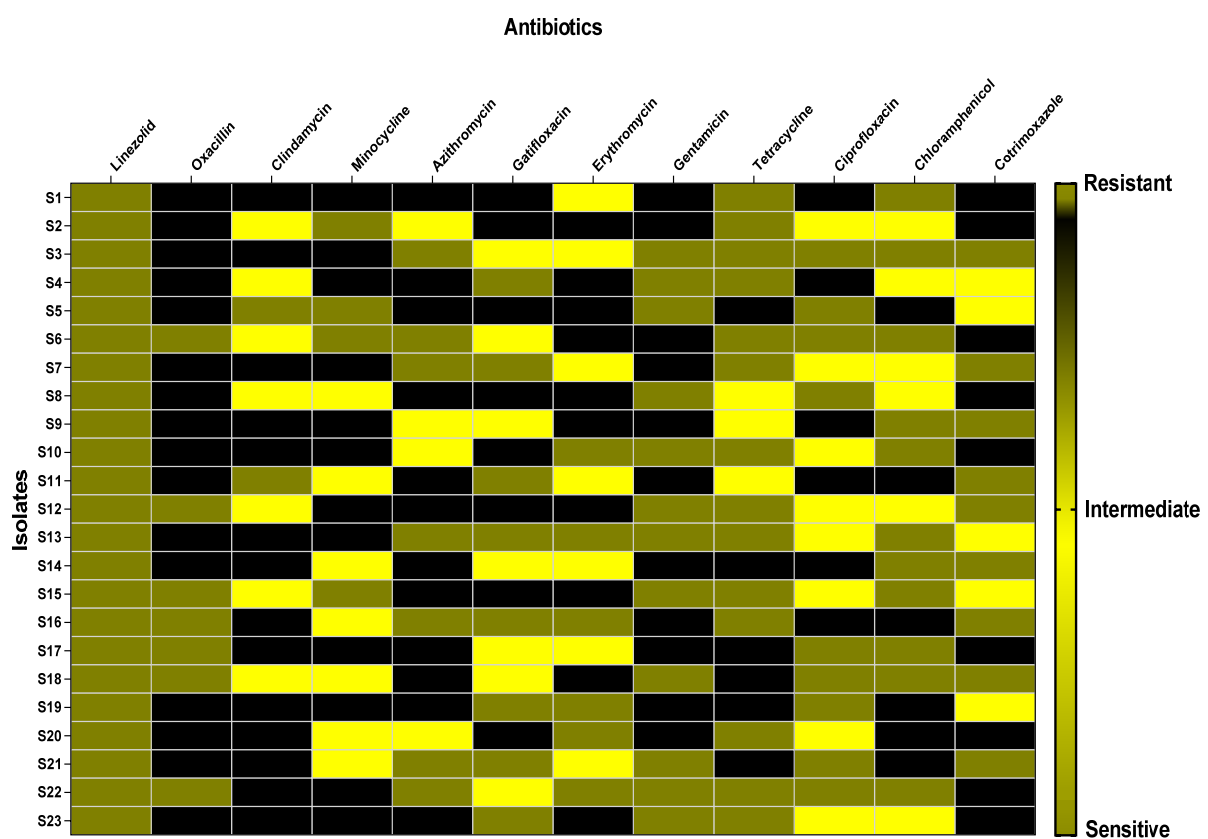


Figure 2. Heat map representing the susceptibility of *S. aureus* isolates to different antibiotics.

2.3. Susceptibility of *S. aureus* to CDE

The susceptibility of *S. aureus* to CDE was elucidated using the agar well diffusion method as a preliminary method to reveal whether CDE possesses antibacterial action (Figure 3 and Table S2). Then, the MICs were determined, as shown in Table S3.

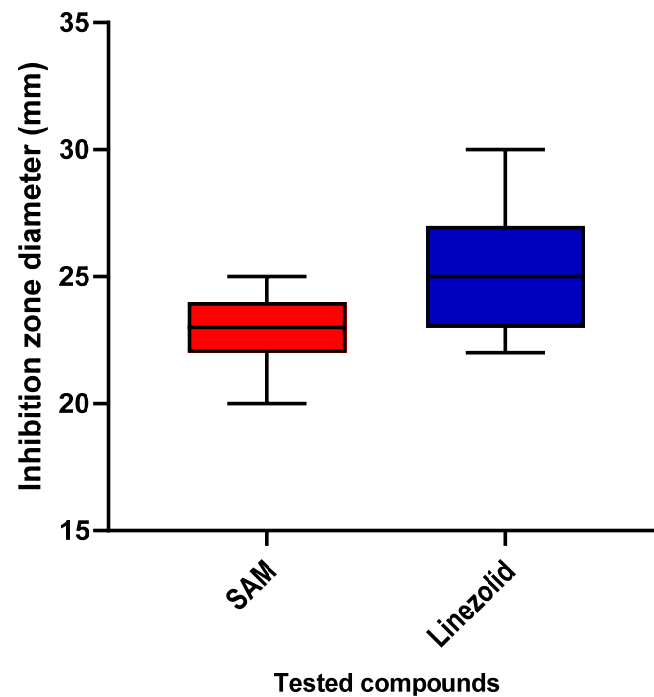


Figure 3. The inhibition zone diameters of CDE against the tested isolates.

2.4. Determination of Antibiofilm Potential by Crystal Violet Assay, SEM, and qRT-PCR

CDE revealed antibiofilm potential through the semiquantitative method, crystal violet (Table 2), as it decreased the percentage of strong and moderate biofilm-forming isolates from 73.91% to 30.43%. Then, SEM was employed to elucidate the effect of CDE on the morphology of the biofilm (Figure 4). CDE has significantly decreased the number of cells in the formed biofilm.

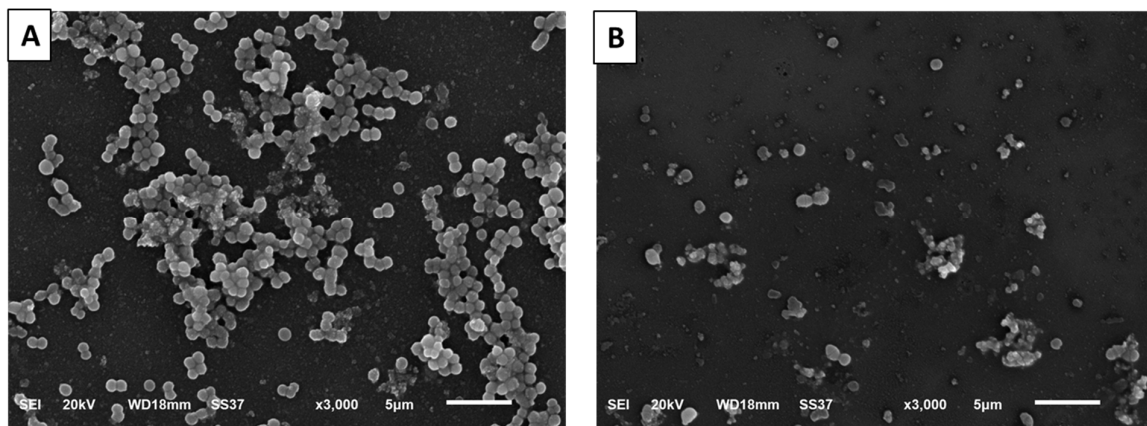


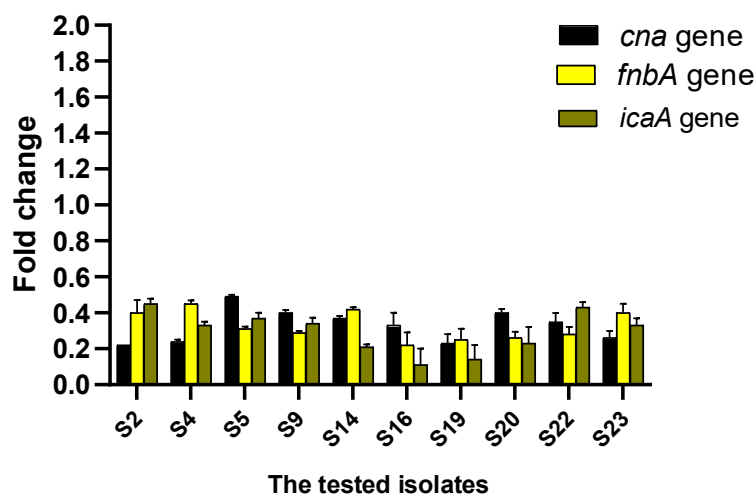
Figure 4. SEM micrograph revealing the morphology of *S. aureus* biofilm formed on the surfaces of cover glass: (A) without (untreated isolates) and (B) with CDE (treated isolates).

qRT-PCR was utilized to reveal the potential of CDE on the expression level of biofilm genes. CDE was found to downregulate the biofilm-encoding genes in 43.48% of the isolates, as revealed in Figure 5.

Table 2. Influence of CDE on the biofilm-forming ability of *S. aureus* isolates.

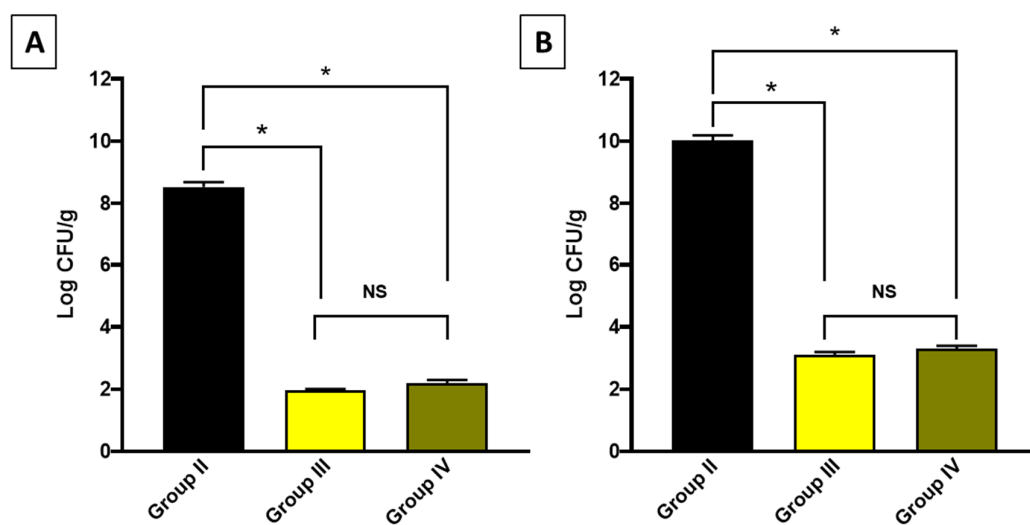
Biofilm Forming Ability *	Number of Isolates	
	Before Treatment	After Treatment
Non-biofilm forming (NBF)	1	5
Weak biofilm forming (WBF)	5	11
Moderate biofilm forming (MBF)	8	3
Strong biofilm forming (SBF)	9	4

* The tested isolates were characterized into four groups based on their ODs as follows: i. NBF: $OD_c < OD < 2 OD_c$. ii. WBF: $2 OD_c < OD < 4 OD_c$. iii. MBPF: $4 OD_c < OD < 6 OD_c$. iv. SBF: $6 OD_c < OD$. The cut-of OD (OD_c) is the mean OD plus 3 SD of the negative control.

**Figure 5.** Impact of CDE on the gene expression levels of the biofilm.

2.5. In Vivo Infection Model in Mice

A systemic infection was induced in mice, and the bacterial burden was detected in the liver and spleen in the experimental groups (Figure 6).

**Figure 6.** Bacterial burden in (A) the liver and (B) the spleen. The symbol (*) denotes a significant difference ($p < 0.05$). The abbreviation (NS) denotes a non-significant difference ($p > 0.05$).

The survival curve was constructed as shown in Figure 7. No mice died in group I; in group II, two died after three days, one after five days, and another after one week. Also,

two mice died after nine days. Regarding groups III and IV, one mouse died on the eighth and sixth days.

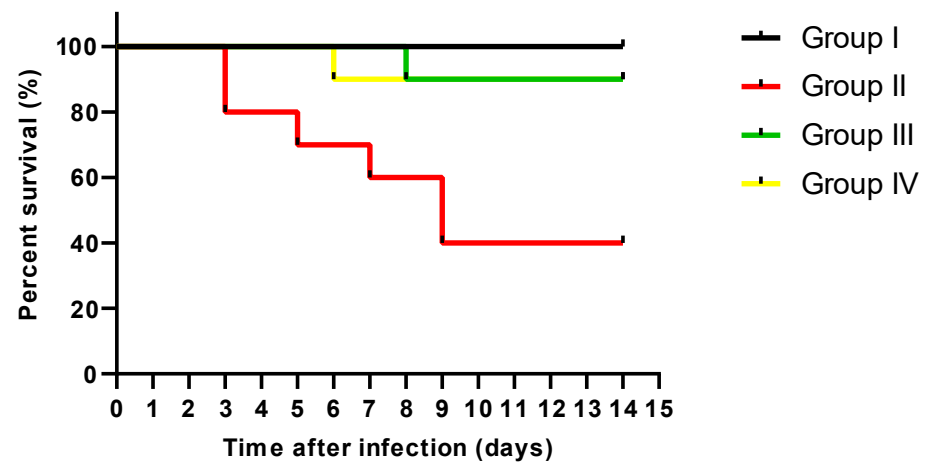


Figure 7. Survival curve constructed for the experimental groups.

2.6. Histopathological and Immunohistochemical Investigations

The effect of CDE on the histological features of the liver and spleen is shown in Figures 8 and 9. Also, the TNF- α immunohistochemical staining of the liver and spleen of the different experimental groups is shown in Figures 10 and 11.

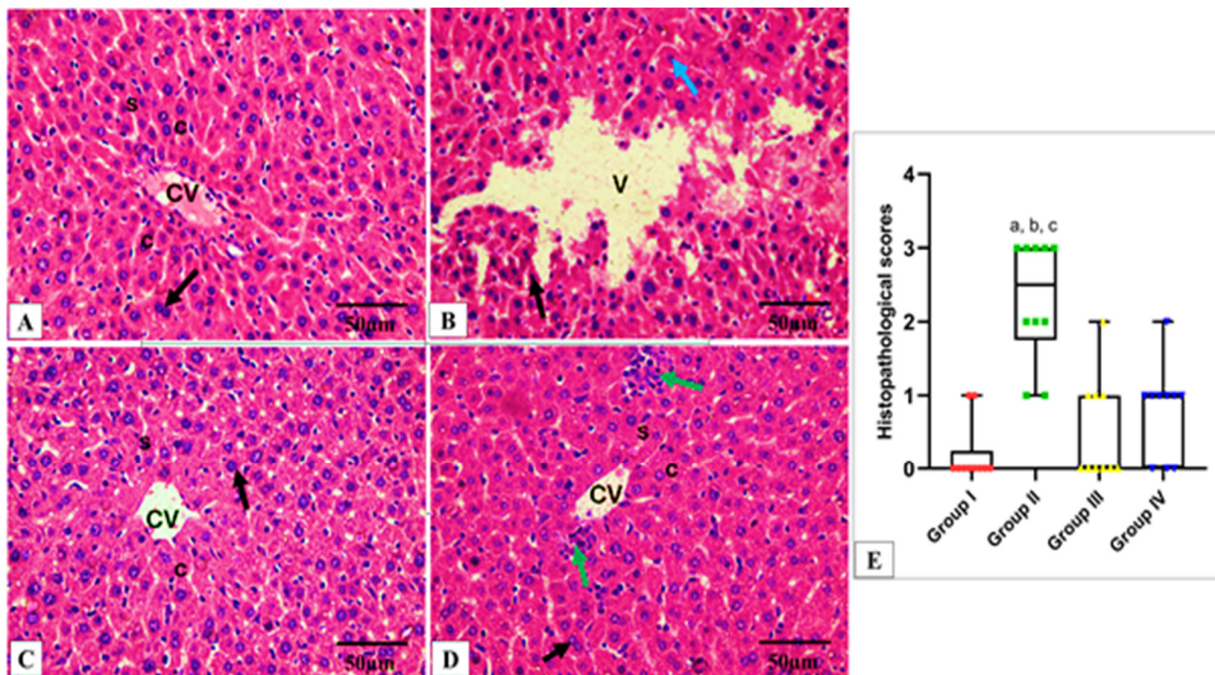


Figure 8. Light microscopic H&E-stained images of hepatic sections of adult albino rats of all studied groups. (A) Group I shows normal hepatic architecture in the form of hepatic cords (c) radiating from the central vein (CV) and separated by the hepatic sinusoids (S), with pericentral zone and midzone hepatocytes. Polyhedral hepatocytes appear with rounded vesicular nuclei and granular eosinophilic cytoplasm (black arrow) separated by sinusoids (S) lined with endothelial cells and Kupffer cells. (B) Group II shows disturbed hepatic architecture, compressed hepatic sinusoids, multiple pyknotic nuclei (black arrow), multiple karyolytic nuclei (blue arrow), and diffuse vacuolar degeneration of hepatocytes with multiple large vacuoles (V) as well as ballooned hepatocytes. (C) Group III shows

organized hepatic cords (C) around the central vein, resembling the normal hepatic structure of Group I. (D) Group IV shows marked improvement and a regaining of the normal hepatic structure. However, with this enhancement, inflammatory cells infiltrate the pericentral zone (green arrow). (E) Histopathological score of the hepatic tissue cross sections in all studied groups. A box plot was used to express the data. The bottom of the plot represents 25%, the middle represents the median, and the top represents 75% of the data. Significant difference at $p \leq 0.05$, where (a) in comparison with group I, (b) in comparison with group III, and (c) in comparison with group IV using the Kruskal–Wallis test followed by Dunn’s pairwise comparison post-hoc test. (H&E $\times 400$, scale bar = 50 μm).

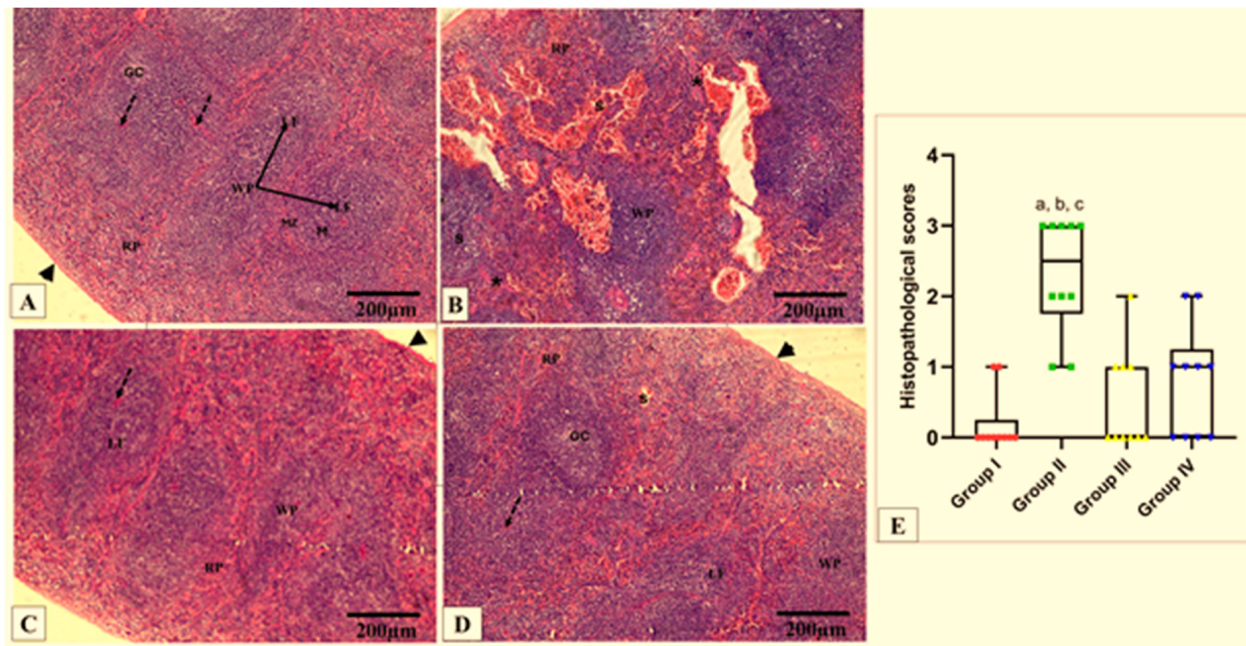


Figure 9. Photomicrographs of H&E-stained sections of spleen in all studied groups. (A) Group I shows the normal histological organization of white pulp (WP) and red pulp (RP) surrounded by a capsule (arrowhead). The WP presents the central arteriole (dashed arrow) and lymphoid follicles (LF), with germinal centers (GC) and mantle regions (M), surrounded by a loosely distributed marginal zone (MZ). The RP presents lymphocytes, trabeculae, and sinusoids. (B) Group II shows a loss of normal architecture, shrunken WP, and broadened RP. Note congested, dilated splenic sinuses (S) in the RP. Many cells in the WP appear vacuolated. Thick fibrous trabeculae are observed (asterisk). (C) Group III shows a nearly normal appearance of the WP and RP splenic architecture. (D) Group IV shows a nearly normal outline of splenic architecture, but congested splenic sinuses are also seen. (E) Histopathological score of the splenic tissue cross sections in all studied groups. A box plot was used to express the data. The bottom of the plot represents 25%, the middle represents the median, and the top represents 75% of the data. Significant difference at $p \leq 0.05$ (a) in comparison with group I, (b) in comparison with group III, and (c) in comparison with group IV using the Kruskal–Wallis test followed by Dunn’s pairwise comparison post-hoc test. (H&E $\times 100$, scale bar = 200 μm).

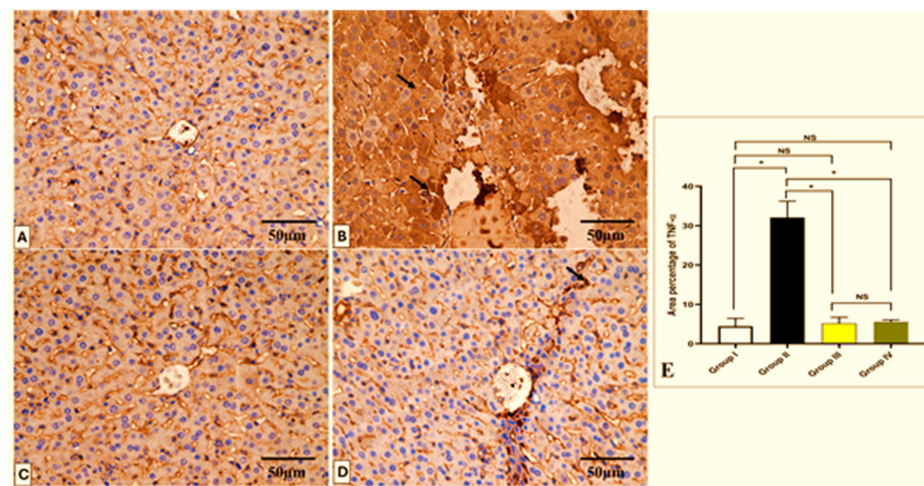


Figure 10. Light microscopic TNF- α -stained pictures of a liver section in all studied groups. (A) Group I shows a negative TNF- α expression within the hepatocytes' cytoplasm. (B) Group II shows a strong positive expression of TNF- α , which appears as brownish cytoplasm in hepatocytes (arrows). (C) Group III shows a negative expression of TNF- α . (D) Group IV shows a mild positive expression of TNF- α in a few hepatocytes (arrow) and a negative expression in most of the cells. (E) The area percentage of TNF- α in each group. Mean \pm SD was used to represent the data. One-way ANOVA was used for the statistical comparison, and Tukey's post-hoc test was used for multiple comparisons. The single asterisk indicates a significant change, and the abbreviation NS denotes a non-significant change ($p < 0.05$). (TNF- α \times 400, scale bar = 50 μ m).

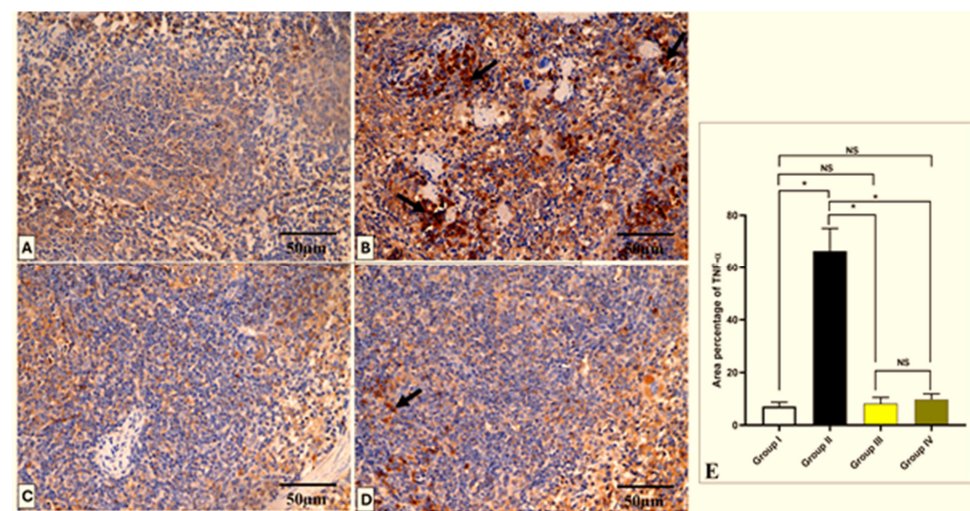


Figure 11. Light microscopic TNF- α -stained pictures of the spleen in all studied groups. (A) Group I shows a negative expression of TNF- α within the cytoplasm of the cells. (B) Group II shows a strong positive expression of TNF- α , which appears as brownish cytoplasm in most cells (arrows). (C) Group III shows a negative expression of TNF- α . (D) Group IV shows few TNF- α -positive cells (arrow) and a negative expression in most cells. (E) The area percentage of TNF- α in each group. Mean \pm SD is used to represent the data. One-way ANOVA was used for the statistical comparison, and Tukey's post-hoc test was used for multiple comparisons. The single asterisk indicates a significant change, and the abbreviation NS denotes a non-significant change ($p < 0.05$). (TNF- α \times 400, scale bar = 50 μ m).

2.7. ELISA

Levels of IL-1 β and IL-6 were detected in the liver and spleen tissues of the different groups (Table 3).

Table 3. Effect of CDE on IL-1 β and IL-6 levels in the liver and spleen of the experimental groups.

Groups	Inflammatory Levels (pg/mg Protein)			
	Liver		Spleen	
	IL-1 β	IL-6	IL-1 β	IL-6
Group I	12.3 \pm 2.3	19.8 \pm 3.2	13.3 \pm 0.8	24.3 \pm 2.5
Group II	80.5 \pm 3.5 *	219.2 \pm 14.5 *	89.3 \pm 7.4 *	240.6 \pm 18.4 *
Group III	19.4 \pm 1.4	28.9 \pm 4.2	20.2 \pm 2.3	34.6 \pm 4.7
Group IV	22.7 \pm 1.1	29.3 \pm 5.3	24.3 \pm 1.4	36.9 \pm 5.8

The symbol (*) denotes a significant difference ($p < 0.05$).

3. Materials and Methods

3.1. Collection, Drying, and Extraction of the Plant Material

The stems, flowers, and leaves of *C. droserifolia* shrubs were collected in March 2022 from the wadis around Sharm El-Sheikh and Dahab in South Sinai Governorate. The plant was dried and powdered to obtain 1.2 kg of dry weight. It was recognized by Prof. Dr. Hanafey Farouk Maswada, Professor of Plant Physiology, Agricultural Botany Department, Faculty of Agriculture, Tanta University, and depositing a voucher specimen (PG-A-00124) in the herbarium of the Department of Pharmacognosy, Faculty of Pharmacy, Tanta University. Methanol (Sigma Chemical Co., St. Louis, MO, USA) was used as an extracting solvent and was mixed with the powder. The extraction was performed thrice (4 L \times 3 times), and then the concentration of the solvent was performed by a rotary evaporator under vacuum to obtain 45.3 g of dry residue from the plant's extract.

3.2. Exploration of the Plant's Phytoconstituents by LC-ESI-MS/MS

Different compounds in the extract were identified by the Proteomics and Metabolomics Unit, Children's Cancer Hospital (57357), Basic Research Department, Cairo, Egypt. The crude extract was reconstituted in DI-Water:Methanol:Acetonitrile—50:25:25, and HPLC separation was accomplished by using in-line filter disks (0.5 μ m \times 3.0 mm, Phenomenex[®], Torrance, CA, USA) and X select HSS T3 (2.5 μ m, 2.1 \times 150 mm, Waters[®], Milford, MA, USA, 40 $^{\circ}$ C). The first is a pre-column, and the second is an analytical column. The mobile phases were composed of mobile phase A, which is composed of 5 mM ammonium formate buffer pH 8 with 1% methanol. Mobile phase B is 100% acetonitrile. Isocratic elution was done using 90% of solvent A and 10% of solvent B for one minute. After that a gradient elution from 90 to 10% solvent A and 10 to 90% of solvent B in twenty minutes was done, then elution with 90% of solvent B for four minutes was done then return to the initial condition (10% of acetonitrile) for three minutes. The flow rate was 0.3 mL/min. The instrument was coupled with Triple TOF 5600+ (Sciex[®], Framingham, MA, USA) for IDA acquisition and Analyst TF 1.7.1 (Sciex[®]) for LC-Triple TOF control. Raw data files were loaded into MS-DIAL 3.52 for data-independent MS/MS deconvolution [69]. Compounds were recognized with >70% probability using an MS1 and MS2 tolerance of 0.2 mass units to be accepted as positive identifications. The ReSpec negative (1573 records) database was used as a reference database. PeakView 2.2 with the MasterView 1.1 package (AB SCIEX, Framingham, MA, USA) were used for feature or peaks extraction from the total ion chromatogram (TIC) based on that the signal-to-noise of features is more than ten, as well as their intensities of the sample-to blank should be more than three [37].

3.3. Bacteria

Twenty-three *S. aureus* isolates were from clinical specimens, including blood, wounds, sputum, and urine. They were identified by standard biochemical tests.

3.4. Antibiotic Susceptibility Testing

The antibiotic sensitivity of the *S. aureus* isolates was explored by the Kirby–Bauer disk diffusion technique. Mueller–Hinton agar (MHA) plates are utilized in this assay [70]. The

following antibiotics were used: oxacillin (OX; 1 µg), erythromycin (E; 15 µg), gentamicin (GN; 10 µg), linezolid (LZD; 30 µg), clindamycin (DA; 2 µg), tetracycline (TE; 30 µg), cotrimoxazole (COT; 1.25/23.75 µg), minocycline (MI; 30 µg), gatifloxacin (GAT; 5 µg), chloramphenicol (C; 30 µg), azithromycin (AZM; 15 µg), and ciprofloxacin (CIP; 5 µg).

3.5. Antibacterial Action of *C. droserifolia* Methanol Extract

Antibacterial action was revealed by agar well diffusion in MHA plates [71]. The bacterial suspension (0.5 McFarland) was dispersed on the surface of the MHA plates. Three wells were performed. The first well-received CDE (2 mg/mL), the second received linezolid (positive control), and the third received dimethyl sulfoxide (DMSO, negative control). The appearance of inhibition zones revealed CDE's antibacterial activity after incubating the plates at 37 °C for 24 h [72].

3.6. Determination of the Minimum Inhibitory Concentration (MIC) of CDE

The broth microdilution assay in MH broth was employed to estimate the MIC values of CDE against *S. aureus* isolates, as previously reported [72]. The MIC had the lowest concentration of CDE, and no growth was detected visually after overnight incubation at 37 °C [73].

3.7. Biofilm Inhibition

The effect of CDE on biofilm formation was investigated at 0.5 MIC values [74]. A tryptone soy broth (TSB) suspension was prepared from an over-night bacterial culture, and was adjusted to 10⁶ CFU/mL in freshly prepared TSB. Then, 200 µL of the bacterial suspension was added to the microtitration plates and wells in the presence and absence of sub-MIC (0.5 MIC) of SAM and incubated at 37 °C for 48 h. The TSB was gently removed, and the wells were washed to remove any planktonic cells and subsequently left for air drying. Add 200 µL of 99% methanol for 20 min, and then the formed biofilm was stained with 200 µL of 1% crystal violet (CV) solution for 15 min. After washing the plate, 33% glacial acetic acid was utilized as a solvent for CV. Using a microtitration plate reader (Sunrise, Männedorf, Switzerland), the absorbance of the solubilized dye was measured at 570 nm [72].

3.8. Scanning Electron Microscope (SEM)

The antibiofilm action of CDE on *S. aureus* bacteria was visualized under SEM, as previously explained (JEOL, Tokyo, Japan) [75].

3.9. Gene Expression Measurement Using qRT-PCR

The influence of CDE on the expression levels of the biofilm genes (*cna*, *fnbA*, and *icaA*) was elucidated using qRT-PCR. After growing the isolates in TSB in the presence and absence of sub-MICs of SAM, they were incubated overnight at 37 °C. After the incubation period, cells were harvested by centrifugation and immediately stored at −80 °C. The total RNA from *S. aureus* isolates was extracted and purified using TRIzol[®] reagent (Life Technologies, Carlsbad, CA, USA) following the manufacturer protocol. Reverse transcription was employed using the QuantiTect Reverse Transcription kit (Qiagen, Hilden, Germany). Then, the formed cDNA was amplified using Maximas SYBR Green/Fluorescein qPCR master mix (Thermo Fisher Scientific, Waltham, MA, USA). The average threshold cycle (CT) values were normalized to the housekeeping gene (16s rRNA). The relative gene expression of the treated isolates was compared to that of the untreated ones according to the 2^{−ΔΔCt} method [76]. Primers are exposed in Table S1 [77,78].

3.10. In Vivo Assay

Forty male mice weighing 25–30 g and aged 6–8 weeks were obtained from the faculty of pharmacy at Tanta University, Egypt. They were grouped into four groups, each with ten mice. The first group was a normal control. The residual three groups

were infected with 0.1 mL via intravenous injection of 1.5×10^7 colony-forming units (CFUs) of *S. aureus* [79]. The second group served as a positive control group (placebo), and the third group administered linezolid (160 mg/kg/24 h) orally as a standard drug. The fourth group administered CDE orally (200 mg/kg/24 h) [12]. The experimental procedures were approved by the ethics committee at the faculty of pharmacy, Tanta University (TP/RE/3/24 p-03).

After two weeks, mice from the diverse groups were euthanized. Liver and spleen samples were obtained from each group. The bacterial burden was determined in the liver and spleen after homogenization. A 1:10 serial dilution of the tissue homogenates in phosphate buffered saline was performed. Then, 100 μ L of undiluted and each subsequent dilution were spread onto tryptic soya agar plates in duplicate using a glass spreader. The plates were then incubated at 37 °C overnight.

The number of colonies was counted on each plate, and the count of CFU/mL was determined as follows: CFU/mL = number of colonies \times dilution factor/0.1 mL. CFU/g = CFU/mL \times number of mL/g [80].

On the other hand, tissue samples (2 \times 3 mm) were excised, fixed in buffered formalin (10%), treated as previously described [81], and finally stained with hematoxylin and eosin (H&E) and photographed using a light microscope. Also, tumor necrosis factor-alpha (TNF- α) monoclonal antibodies were utilized for staining the tissues. The immunostained tissues were then checked by a light microscope.

3.11. ELISA

The anti-inflammatory potential of CDE was illuminated by determining the levels of the inflammatory mediators, interleukin IL-1 β and IL-6 in pg/mg protein in the liver and spleen tissues by an ELISA kit from Abcam Co., Waltham, MA, USA, following the manufacturer's instructions.

3.12. Histopathological Examination

Formalin-fixed hepatic and splenic tissues were processed, and 5- μ m-thick paraffin sections were stained with hematoxylin and eosin (H&E). Photomicrographs were taken at different magnification powers using a light microscope (Olympus, Tokyo, Japan) to assess the morphological changes [82]. Histopathological evaluation of the hepatic and splenic tissue damage was performed. A score of zero indicates the absence of tissue necrosis; a score of one indicates mild damage, 10–20% liver cell degeneration, necrosis, and 10–20% red blood cell depletion. A score of two indicates moderate degeneration in the form of 20–40% liver cell degeneration, necrosis, and 20–40% red blood cell depletion in the spleen. A score of three indicates severe degeneration in the form of >40% liver cell degeneration and necrosis and >40% red blood cell depletion in the spleen.

3.13. Immunohistochemistry

Six-micrometer tissue sections from the liver and spleen were subjected to immunohistochemical staining; they were first dewaxed, rehydrated by a diminishing alcohol series, and treated with 10% hydrogen peroxide in methanol for ten minutes. Following this, the sections were microwaved for ten minutes in 0.01 M sodium citrate buffer (pH 6.0), allowed to cool at room temperature, and then repeatedly washed with PBS for five minutes. After washing, antigens were recovered by autoclaving in citrate buffer for 11 min. Next, slices were incubated with primary antibodies for a whole night at 4 °C. Then, the tissues were treated for 30 min at room temperature with 3, 3-diaminobenzidine and a rabbit polyclonal TNF- α antibody. The tissue sections were mounted for visibility, washed in xylene, and subtly counterstained with hematoxylin. Slides were examined under a light microscope at a magnification of \times 400 [83]. Using image analysis tools (Image J, 1.46a, NIH, Bethesda, MD, USA), morphometric analysis was carried out. At \times 400 magnification, the mean area percentage of TNF- α protein expression for each of the experimental groups was evaluated in ten non-overlapping fields within each region.

3.14. Statistics

The assays were carried out three times and exposed as mean \pm standard deviation (SD). ANOVA was utilized to reveal the significance of differences among the experimental groups by GraphPad software version 8.0 (GraphPad Software, LLC, Boston, MA, USA). Results of the histopathological scores were analyzed using Kruskal–Wallis test followed by Dunn’s multiple comparison test.

4. Discussion

Medicinal plants can act as a natural source of numerous therapeutic compounds that can be utilized safely to treat various diseases in humans and animals [84]. In recent decades, increasing attention has been paid to elucidating plants as an important source for numerous drugs, principally antimicrobials, to combat multidrug-resistant bacteria [85]. Here, the tested *S. aureus* isolates were from blood (52.17%), wounds (21.73%), sputum (17.4%), and urine (8.7%). Previous studies have documented that most recovered *S. aureus* isolates were from blood and wounds [86–88]. Regarding the susceptibility to antibiotics, the isolates tested in our study revealed multidrug resistance comparable to previous reports [89–91].

CDE revealed antibacterial action on *S. aureus* isolates with MIC values of 128–512 $\mu\text{g}/\text{mL}$. An earlier study described the antibacterial action of CDE on *S. aureus* NCTC 10788, *Salmonella senftenberg* ATCC 8400, *Escherichia coli* BA 12296, and *Candida albicans* ATCC MAY-2876 [12]. In addition, the antibacterial action of the essential oil obtained from *Cleome* species was previously reported on Gram-positive and Gram-negative bacterial species [92].

The phytochemical analysis by LC-ESI-MS/MS of *C. droserifolia* methanol extract tentatively identified 44 compounds belonging to different entities. Flavonoids, anthocyanin, and organic acids composed a major part of the extract, and it was found that the major constituents were kaempferol-3,7-*O*-bis- α -L-rhamnoside, isorhamnetin, cyanidin-3-glucoside, 3, 5, 7-trihydroxy-4'-methoxyflavone (kaempferide), kaempferol-3-*O*- α -L-rhamnoside, caffeic acid, isoquercitrin, quinic acid, isocitrate, mannitol, apigenin, acacetin, and naringenin. Kaempferol glycosides were reported to exert antimicrobial and anti-inflammatory effects [93,94]. Isorhamnetin, or 3'-methoxylated quercetin derivative, is a flavanol with antidiabetic, anti-inflammatory, and antimicrobial effects [95]. Flavonoids such as kaempferol derivatives, isorhamnetin, apigenin, acacetin, and naringenin are valuable groups of compounds with antimicrobial and anti-biofilm activities [96].

Wang et al. reported that cyanidin-3-glucoside exhibited antimicrobial and anti-inflammatory potential [97]. Cyanidin-3-glucoside inhibits the NF- κ B pathway. Also, it was reported to inhibit the interferon-mediated inflammatory cascades and reduce the proinflammatory cytokines, such as interferon- γ , TNF- α , interleukin (IL)-5, IL-9, and IL-10 [95,98].

As biofilm is an important virulence factor for *S. aureus*, it enables it to resist multiple antibiotics by transferring the genes of resistance among the bacterial cells embedded in the biofilms and by hindering the penetration of the antibiotics across the biofilm [99,100]. Thus, antibiofilm agents are beneficial for managing MDR *S. aureus* infections [101]. Herein, CDE revealed antibiofilm action by crystal violet and SEM. Also, it revealed a downregulating effect on the biofilm-encoding genes (*cna*, *fnbA*, and *icaA*) using qRT-PCR in 43.48% of the isolates. Such genes encode intracellular adhesion molecules (*icaA*) and microbial surface components recognizing adhesive matrix molecules (*fnbA* and *cna*), which have a great role in biofilm formation [102].

Regarding the *in vivo* model, which was employed to simulate the human body [103], CDE revealed a promising effect in the studied infection model as it significantly decreased the bacterial count in the liver and spleen, indicating its antibacterial action *in vivo*. Also, it improved the histological features of the liver and spleen, manifested by regaining the normal hepatic structure and the splenic architecture.

As bacterial infections are among the causes that often trigger inflammation as a body response [104], we elucidated the consequence of CDE on the inflammatory markers in the liver and spleen using immunohistochemistry and ELISA. TNF- α is an inflammatory cytokine produced by macrophages as a response to acute inflammation [105,106]. Also, IL-1 β is a proinflammatory cytokine that mediates numerous physiological responses, such as fever and lymphocyte activation [107,108]. IL-6 is an important pleiotropic cytokine in the inflammatory response [109–111]. Remarkably, CDE has significantly diminished these inflammatory mediators, which could have a role in its antibacterial potential. The experiment demonstrated a notable enhancement in the survival rate of rats infected with *S. aureus* when treated with CDE compared to the positive control group. CDE efficacy was comparable to that of the standard drug, linezolid. These results highlight the potential therapeutic value of CDE as an alternative treatment for *S. aureus* infections, warranting further investigation into the clinical relevance of these findings.

5. Conclusions

LC-ESI-MS/MS revealed that *C. droserifolia* methanol extract had variable phytochemicals with valuable biological activities. Flavonoid glycosides, anthocyanins, and other phenolic compounds were believed to cause multiple effects, such as antimicrobial, antibiofilm, and anti-inflammatory properties. The predominant compounds in CDE were kaempferol-3,7-*O*-bis- α -L-rhamnoside, isorhamnetin, cyanidin-3-glucoside, 3, 5, 7-trihydroxy-4'-methoxyflavone (kaempferide), kaempferol-3-*O*- α -L-rhamnoside, caffeic acid, isoquercitrin, quinic acid, isocitrate, mannitol, apigenin, acacetin, and naringenin. CDE exhibited a potent antibacterial action on *S. aureus* isolates with MICs that ranged from 128 to 512 μ g/mL. It also revealed antibiofilm action using a crystal violet assay and SEM. This antibiofilm potential was further studied at the molecular level using qRT-PCR on the biofilm-encoding genes, and it revealed a downregulating action on the studied genes in 43.48% of the isolates. In the *in vivo* aspect, using ELISA and immunohistochemical studies, the CDE-treated group showed a significant improvement in the histological features, with a significant lessening in the inflammatory markers in the liver and spleen. Our work has shown that treatment with CDE can significantly improve the survival rate of *S. aureus*-infected rats, with efficacy similar to that of the standard drug linezolid, suggesting potential therapeutic value and prompting further exploration of its clinical relevance. Thus, it is important to perform future studies on CDE to reveal its potential activity on other bacterial species and to elucidate its action in clinical practice.

Supplementary Materials: The following supporting information can be downloaded at: <https://www.mdpi.com/article/10.3390/antibiotics13050450/s1>, Table S1. Sequences of the utilized primers. Table S2. Inhibition zone diameter of SAM, linezolid (positive control), and DMSA (negative control). Table S3. Minimum inhibitory concentrations (MICs) of SAM. Figure S1. Negative mode total ion chromatogram of LC-ESI-MS/MS of *Cleome droserifolia* methanol extract.

Author Contributions: J.A.: data curation, funding acquisition, software, validation, and writing—review and editing. W.A.N.: data curation, formal analysis, methodology, writing—original draft, and writing—review and editing. E.E.: data curation, formal analysis, methodology, writing—original draft, and writing—review and editing. I.A.H.: funding acquisition, investigation, resources, software, and writing—review and editing. H.S.H.: resources, software, validation, and writing—original draft. A.R.A.: funding acquisition, investigation, resources, and software. E.M.: data curation, project administration, resources, validation, and writing—review and editing. R.A.: data curation, investigation, software, validation, and writing—review and editing. S.I.: methodology, software, and writing—original draft. S.A.E.-S.: data curation, formal analysis, methodology, writing—original draft, and writing—review and editing. All authors have read and agreed to the published version of the manuscript.

Funding: This research received funding from Researchers Supporting Project number (RSPD2024R583), King Saud University, Riyadh, Saudi Arabia.

Institutional Review Board Statement: The experimental procedures were approved by the ethics committee at the faculty of pharmacy, Tanta University (TP/RE/3/24 p-03).

Informed Consent Statement: Not applicable.

Data Availability Statement: Data are contained within the article and Supplementary Materials.

Acknowledgments: The authors are thankful to Researchers Supporting Project number (RSPD2024R583), King Saud University, Riyadh, Saudi Arabia.

Conflicts of Interest: The authors declare absence of conflict of interests.

References

1. Moustafa, A.A.; Mahmoud, M.A.K. Importance of *Cleome droserifolia* as an endangered medicinal plant species in the Sinai Peninsula and the need for its conservation. *Adv. Med. Plant Res.* **2023**, *11*, 43–51.
2. Hegazy, A.K. Population ecology and implications for conservation of *Cleome droserifolia*: A threatened xerophyte. *J. Arid Environ.* **1990**, *19*, 269–282. [[CrossRef](#)]
3. a Moustafa, A.R.; Alotaibi, M.O. *Cleome droserifolia*: An Egyptian natural heritage facing extinction. *Asian J. Plant Sci. Res.* **2019**.
4. Darbyshire, I.; Kordofani, M.; Farag, I.; Candiga, R.; Pickering, H. *The Plants of Sudan and South Sudan: An Annotated Checklist*; Royal Botanic Gardens: Kew, UK, 2015.
5. Ghazanfar, S.A. *An Annotated Catalogue of the Vascular Plants of Oman and Their Vernacular Names*; Jardin Botanique National de Belgique: Meise, Belgium, 1992; Volume 2.
6. Batanouny, K.; Aboutabl, E.; Shabana, M.; Soliman, F. *Wild Medicinal Plants in Egypt*; The Palm Press: Cairo, Egypt, 1999; Volume 154.
7. Tackholm, V.; Boulos, L. *Students' Flora of Egypt*; Cairo University: Cairo, Egypt, 1974.
8. El-Askary, H.I. Terpenoids from *Cleome droserifolia* (Forssk.) Del. *Molecules* **2005**, *10*, 971–977. [[CrossRef](#)] [[PubMed](#)]
9. Helal, E.G.; Khattab, A.M.; Abou Aouf, N.; Abdallah, I.Z. Hypoglycemic and antioxidant effects of *Cleome droserifolia* (Samwah) in Alloxan-induced diabetic rats. *Egypt. J. Hosp. Med.* **2015**, *58*, 39–47. [[CrossRef](#)]
10. Seif El-Din, A.; Darwish, F.; Abou-Donia, A. Flavonoids from *Cleome droserifolia* (Forssk.) Del. Growing in Egypt. *Egypt. J. Pharm. Sci.* **1987**, *28*, 313.
11. Abd El-Gawad, A.M.; El-Amier, Y.A.; Bonanomi, G. Essential oil composition, antioxidant and allelopathic activities of *Cleome droserifolia* (Forssk.) Delile. *Chem. Biodivers.* **2018**, *15*, e1800392. [[CrossRef](#)] [[PubMed](#)]
12. Hashem, N.M.; Shehata, M.G. Antioxidant and antimicrobial activity of *Cleome droserifolia* (Forssk.) Del. and its biological effects on redox status, immunity, and gut microflora. *Animals* **2021**, *11*, 1929. [[CrossRef](#)] [[PubMed](#)]
13. Abdel-Latif, M.; Riad, A.; Soliman, R.A.; Elkhoully, A.M.; Nafae, H.; Gad, M.Z.; Motaal, A.A.; Youness, R.A. MALAT-1/p53/miR-155/miR-146a ceRNA circuit tuned by methoxylated quercetin glycoside alters immunogenic and oncogenic profiles of breast cancer. *Mol. Cell. Biochem.* **2022**, *477*, 1281–1293. [[CrossRef](#)]
14. Nicola, W.; Ibrahim, K.; Mikhail, T.; Girgis, R.; Khadr, M. Role of the hypoglycemic plant extract *cleome droserifolia* in improving glucose and lipid metabolism and its relation to insulin resistance in fatty liver. *Boll. Chim. Farm.* **1996**, *135*, 507–517.
15. Cave, R.; Misra, R.; Chen, J.; Wang, S.; Mkrtychyan, H.V. Whole genome sequencing revealed new molecular characteristics in multidrug resistant staphylococci recovered from high frequency touched surfaces in London. *Sci. Rep.* **2019**, *9*, 9637. [[CrossRef](#)]
16. Cepas, V.; Soto, S.M. Relationship between virulence and resistance among gram-negative bacteria. *Antibiotics* **2020**, *9*, 719. [[CrossRef](#)]
17. Cheung, G.Y.; Bae, J.S.; Otto, M. Pathogenicity and virulence of *Staphylococcus aureus*. *Virulence* **2021**, *12*, 547–569. [[CrossRef](#)]
18. Kakoullis, L.; Papachristodoulou, E.; Chra, P.; Panos, G. Mechanisms of antibiotic resistance in important gram-positive and gram-negative pathogens and novel antibiotic solutions. *Antibiotics* **2021**, *10*, 415. [[CrossRef](#)] [[PubMed](#)]
19. Saha, M.; Sarkar, A. Review on multiple facets of drug resistance: A rising challenge in the 21st century. *J. Xenobiotics* **2021**, *11*, 197–214. [[CrossRef](#)] [[PubMed](#)]
20. Idrees, M.; Sawant, S.; Karodia, N.; Rahman, A. *Staphylococcus aureus* biofilm: Morphology, genetics, pathogenesis and treatment strategies. *Int. J. Environ. Res. Public Health* **2021**, *18*, 7602. [[CrossRef](#)] [[PubMed](#)]
21. Yin, W.; Wang, Y.; Liu, L.; He, J. Biofilms: The microbial “protective clothing” in extreme environments. *Int. J. Mol. Sci.* **2019**, *20*, 3423. [[CrossRef](#)] [[PubMed](#)]
22. Muteeb, G.; Rehman, M.T.; Shahwan, M.; Aatif, M. Origin of antibiotics and antibiotic resistance, and their impacts on drug development: A narrative review. *Pharmaceuticals* **2023**, *16*, 1615. [[CrossRef](#)]
23. Siddiqui, S.A.; Khan, S.; Mehdizadeh, M.; Bahmid, N.A.; Adli, D.N.; Walker, T.R.; Perestrelo, R.; Câmara, J.S. Phytochemicals and bioactive constituents in food packaging: A systematic review. *Heliyon* **2023**, *9*, e21196. [[CrossRef](#)]
24. Bittner Fialová, S.; Rendeková, K.; Mučaji, P.; Nagy, M.; Slobodníková, L. Antibacterial activity of medicinal plants and their constituents in the context of skin and wound infections, considering European legislation and folk medicine—A review. *Int. J. Mol. Sci.* **2021**, *22*, 10746. [[CrossRef](#)]

25. Attallah, N.G.; Al-Fakhrany, O.M.; Elekhrawy, E.; Hussein, I.A.; Shaldam, M.A.; Altwajry, N.; Alqahtani, M.J.; Negm, W.A. Anti-Biofilm and Antibacterial Activities of *Cycas media* R. Br Secondary Metabolites: *In Silico*, *In Vitro*, and *In Vivo* Approaches. *Antibiotics* **2022**, *11*, 993. [[CrossRef](#)] [[PubMed](#)]
26. Alherz, F.A.; Negm, W.A.; Elekhrawy, E.; El-Masry, T.A.; Haggag, E.M.; Alqahtani, M.J.; Hussein, I.A. Silver Nanoparticles Prepared Using *Encephalartos laurentianus* De Wild Leaf Extract Have Inhibitory Activity against *Candida albicans* Clinical Isolates. *J. Fungi* **2022**, *8*, 1005. [[CrossRef](#)]
27. Negm, W.A.; El-Aasr, M.; Attia, G.; Alqahtani, M.J.; Yassien, R.I.; Abo Kamer, A.; Elekhrawy, E. Promising Antifungal Activity of *Encephalartos laurentianus* de Wild against *Candida albicans* Clinical Isolates: *In Vitro* and *In Vivo* Effects on Renal Cortex of Adult Albino Rats. *J. Fungi* **2022**, *8*, 426. [[CrossRef](#)] [[PubMed](#)]
28. Alqahtani, M.J.; Elekhrawy, E.; Negm, W.A.; Mahgoub, S.; Hussein, I.A. *Encephalartos villosus* Lem. Displays a strong *in vivo* and *in vitro* antifungal potential against *Candida glabrata* clinical isolates. *J. Fungi* **2022**, *8*, 521. [[CrossRef](#)] [[PubMed](#)]
29. Motaal, A.A.; Ezzat, S.M.; Haddad, P. Determination of bioactive markers in *Cleome droserifolia* using cell-based bioassays for antidiabetic activity and isolation of two novel active compounds. *Phytomedicine* **2011**, *19*, 38–41. [[CrossRef](#)] [[PubMed](#)]
30. Jarukas, L.; Kamarauskaite, J.; Marksa, M.; Trumbeckaitė, S.; Baniene, R.; Ivanauskas, L. Bio-based succinic acid sample preparation and derivatization procedure optimisation for gas chromatography-mass spectrometry analysis. *Sci. Pharm. Sci.* **2018**, *4*, 9–13. [[CrossRef](#)]
31. Vasilev, H.; Šmejkal, K.; Jusková, S.; Vaclavik, J.; Tremel, J. Five New Tamarixetin Glycosides from *Astragalus thracicus* Griseb. Including Some Substituted with the Rare 3-Hydroxy-3-methylglutaric Acid and Their Collagenase Inhibitory Effects *In Vitro*. *ACS Omega* **2024**, *9*, 18023–18031. [[CrossRef](#)]
32. Abela, L.; Spiegel, R.; Crowther, L.M.; Klein, A.; Steindl, K.; Papuc, S.M.; Joset, P.; Zehavi, Y.; Rauch, A.; Plecko, B. Plasma metabolomics reveals a diagnostic metabolic fingerprint for mitochondrial aconitase (ACO2) deficiency. *PLoS ONE* **2017**, *12*, e0176363. [[CrossRef](#)] [[PubMed](#)]
33. Shahzad, M.N.; Ahmad, S.; Tousif, M.I.; Ahmad, I.; Rao, H.; Ahmad, B.; Basit, A. Profiling of phytochemicals from aerial parts of *Terminalia neotaliala* using LC-ESI-MS² and determination of antioxidant and enzyme inhibition activities. *PLoS ONE* **2022**, *17*, e0266094. [[CrossRef](#)]
34. Surendra, S.V.; Mahalingam, B.L.; Velan, M. Degradation of monoaromatics by *Bacillus pumilus* MVSV3. *Braz. Arch. Biol. Technol.* **2017**, *60*, e16160319. [[CrossRef](#)]
35. Mekky, R.H.; del Mar Contreras, M.; El-Gindi, M.R.; Abdel-Monem, A.R.; Abdel-Sattar, E.; Segura-Carretero, A. Profiling of phenolic and other compounds from Egyptian cultivars of chickpea (*Cicer arietinum* L.) and antioxidant activity: A comparative study. *RSC Adv.* **2015**, *5*, 17751–17767. [[CrossRef](#)]
36. Mahrous, F.S.M.; Mohammed, H.; Sabour, R. LC-ESI-QTOF-MS/MS of *Holoptelea integrifolia* (Roxb.) Planch. leaves and *In silico* study of phenolic compounds' antiviral activity against the HSV1 virus. *Azhar Int. J. Pharm. Med. Sci.* **2021**, *1*, 91–101. [[CrossRef](#)]
37. Attallah, N.G.; Negm, W.A.; Elekhrawy, E.; Elmongy, E.I.; Altwajry, N.; El-Haroun, H.; El-Masry, T.A.; El-Sherbeni, S.A. Elucidation of phytochemical content of *Cupressus macrocarpa* leaves: *In Vitro* and *in vivo* antibacterial effect against methicillin-resistant *Staphylococcus aureus* clinical isolates. *Antibiotics* **2021**, *10*, 890. [[CrossRef](#)]
38. Simirgiotis, M.J.; Schmeda-Hirschmann, G. Direct identification of phenolic constituents in Boldo Folium (*Peumus boldus* Mol.) infusions by high-performance liquid chromatography with diode array detection and electrospray ionization tandem mass spectrometry. *J. Chromatogr. A* **2010**, *1217*, 443–449. [[CrossRef](#)]
39. Huang, G.; Liang, J.; Chen, X.; Lin, J.; Wei, J.; Huang, D.; Zhou, Y.; Sun, Z.; Zhao, L. Isolation and identification of chemical constituents from zhideke granules by ultra-performance liquid chromatography coupled with mass spectrometry. *J. Anal. Methods Chem.* **2020**, *2020*, 8889607. [[CrossRef](#)]
40. Li, W.; Sun, Y.; Liang, W.; Fitzloff, J.F.; van Breemen, R.B. Identification of caffeic acid derivatives in *Actea racemosa* (*Cimicifuga racemosa*, black cohosh) by liquid chromatography/tandem mass spectrometry. *Rapid Commun. Mass Spectrom.* **2003**, *17*, 978–982. [[CrossRef](#)]
41. Ferreira, P.S.; Victorelli, F.D.; Fonseca-Santos, B.; Chorilli, M. A review of analytical methods for p-coumaric acid in plant-based products, beverages, and biological matrices. *Crit. Rev. Anal. Chem.* **2019**, *49*, 21–31. [[CrossRef](#)]
42. Andini, S.; Dekker, P.; Gruppen, H.; Araya-Cloutier, C.; Vincken, J.-P. Modulation of glucosinolate composition in Brassicaceae seeds by germination and fungal elicitation. *J. Agric. Food Chem.* **2019**, *67*, 12770–12779. [[CrossRef](#)]
43. Wang, Y.; Zhao, M.; Ou, Y.; Zeng, B.; Lou, X.; Wang, M.; Zhao, C. Metabolic profile of esculin in rats by ultra high performance liquid chromatography combined with Fourier transform ion cyclotron resonance mass spectrometry. *J. Chromatogr. B* **2016**, *1020*, 120–128. [[CrossRef](#)]
44. Jaiswal, R.; Müller, H.; Müller, A.; Karar, M.G.E.; Kuhnert, N. Identification and characterization of chlorogenic acids, chlorogenic acid glycosides and flavonoids from *Lonicera henryi* L. (Caprifoliaceae) leaves by LC-MSⁿ. *Phytochemistry* **2014**, *108*, 252–263. [[CrossRef](#)]
45. Razgonova, M.; Zakharenko, A.; Pikula, K.; Manakov, Y.; Ercisli, S.; Derbush, I.; Kislin, E.; Seryodkin, I.; Sabitov, A.; Kalenik, T. LC-MS/MS Screening of Phenolic Compounds in Wild and Cultivated Grapes *Vitis amurensis* Rupr. *Molecules* **2021**, *26*, 3650. [[CrossRef](#)]

46. El-Newary, S.A.; Abd Elkarim, A.S.; Abdelwahed, N.A.; Omer, E.A.; Elgamal, A.M.; Elsayed, W.M. *Chenopodium murale* Juice Shows Anti-Fungal Efficacy in Experimental Oral Candidiasis in Immunosuppressed Rats in Relation to Its Chemical Profile. *Molecules* **2023**, *28*, 4304. [[CrossRef](#)]
47. Feketeová, L.; Barlow, C.K.; Benton, T.M.; Rochfort, S.J.; Richard, A. The formation and fragmentation of flavonoid radical anions. *Int. J. Mass Spectrom.* **2011**, *301*, 174–183. [[CrossRef](#)]
48. Schütz, K.; Persike, M.; Carle, R.; Schieber, A. Characterization and quantification of anthocyanins in selected artichoke (*Cynara scolymus* L.) cultivars by HPLC–DAD–ESI–MSⁿ. *Anal. Bioanal. Chem.* **2006**, *384*, 1511–1517. [[CrossRef](#)]
49. Sánchez-Ilárduya, M.; Sánchez-Fernández, C.; Vilorio-Bernal, M.; López-Márquez, D.; Berrueta, L.; Gallo, B.; Vicente, F. Mass spectrometry fragmentation pattern of coloured flavanol-anthocyanin and anthocyanin-flavanol derivatives in aged red wines of Rioja. *Aust. J. Grape Wine Res.* **2012**, *18*, 203–214. [[CrossRef](#)]
50. Abdl Aziz, F.T.; Temraz, A.S.; Hassan, M.A. Metabolites profiling by LC-ESI-MS/MS technique and in-vitro antioxidant activity of *Bauhinia madagascariensis* Desv. and *Bauhinia purpurea* L. aerial parts cultivated in Egypt: A comparative study. *Azhar Int. J. Pharm. Med. Sci.* **2024**, *4*, 169–188. [[CrossRef](#)]
51. Siger, A.; Czubinski, J.; Dwiecki, K.; Kachlicki, P.; Nogala-Kalucka, M. Identification and antioxidant activity of sinapic acid derivatives in *Brassica napus* L. seed meal extracts. *Eur. J. Lipid Sci. Technol.* **2013**, *115*, 1130–1138. [[CrossRef](#)]
52. Asen, S.; Plimmer, J.R. 4,6,4'-Trihydroxyaurone and other flavonoids from Limonium. *Phytochemistry* **1972**, *11*, 2601–2603. [[CrossRef](#)]
53. Mizuno, T.; Uchiyama, N.; Tanaka, S.; Nakane, T.; Devkota, H.P.; Fujikawa, K.; Kawahara, N.; Iwashina, T. Flavonoids from *Sedum japonicum* subsp. *oryzifolium* (Crassulaceae). *Molecules* **2022**, *27*, 7632. [[CrossRef](#)]
54. Hu, Q.; Sun, Y.; Mu, X.; Wang, Y.; Tang, H. Reliable quantification of citrate isomers and isobars with direct-infusion tandem mass spectrometry. *Talanta* **2023**, *259*, 124477. [[CrossRef](#)]
55. Zhou, Y.; Li, P.; Brantner, A.; Wang, H.; Shu, X.; Yang, J.; Si, N.; Han, L.; Zhao, H.; Bian, B. Chemical profiling analysis of Maca using UHPLC-ESI-Orbitrap MS coupled with UHPLC-ESI-QqQ MS and the neuroprotective study on its active ingredients. *Sci. Rep.* **2017**, *7*, 44660. [[CrossRef](#)]
56. Ablajan, K.; Tuoheti, A. Fragmentation characteristics and isomeric differentiation of flavonol O-rhamnosides using negative ion electrospray ionization tandem mass spectrometry. *Rapid Commun. Mass Spectrom.* **2013**, *27*, 451–460. [[CrossRef](#)]
57. Rini Vijayan, K.P.; Raghu, A. Tentative characterization of phenolic compounds in three species of the genus *Embelia* by liquid chromatography coupled with mass spectrometry analysis. *Spectrosc. Lett.* **2019**, *52*, 653–670. [[CrossRef](#)]
58. Brito, A.; Areche, C.; Sepúlveda, B.; Kennelly, E.J.; Simirgiotis, M.J. Anthocyanin characterization, total phenolic quantification and antioxidant features of some Chilean edible berry extracts. *Molecules* **2014**, *19*, 10936–10955. [[CrossRef](#)]
59. Abd-El-Aziz, N.M.; Hifnawy, M.S.; Lotfy, R.A.; Younis, I.Y. LC/MS/MS and GC/MS/MS metabolic profiling of *Leontodon hispidulus*, *in vitro* and *in silico* anticancer activity evaluation targeting hexokinase 2 enzyme. *Sci. Rep.* **2024**, *14*, 6872. [[CrossRef](#)]
60. Kaur, J.; Dhiman, V.; Bhadada, S.; Katare, O.; Ghoshal, G. LC/MS guided identification of metabolites of different extracts of *Cissus quadrangularis*. *Food Chem. Adv.* **2022**, *1*, 100084. [[CrossRef](#)]
61. Brito, A.; Ramirez, J.E.; Areche, C.; Sepúlveda, B.; Simirgiotis, M.J. HPLC-UV-MS profiles of phenolic compounds and antioxidant activity of fruits from three citrus species consumed in Northern Chile. *Molecules* **2014**, *19*, 17400–17421. [[CrossRef](#)]
62. Choi, S.S.; Lee, S.H.; Lee, K.A. A Comparative Study of Hesperetin, Hesperidin and Hesperidin Glucoside: Antioxidant, Anti-Inflammatory, and Antibacterial Activities *In Vitro*. *Antioxidants* **2022**, *11*, 1618. [[CrossRef](#)]
63. Wu, W.; Liu, Z.; Song, F.; Liu, S. Structural analysis of selected characteristic flavones by electrospray tandem mass spectrometry. *Anal. Sci.* **2004**, *20*, 1103–1105. [[CrossRef](#)]
64. Fabre, N.; Rustan, I.; de Hoffmann, E.; Quetin-Leclercq, J. Determination of flavone, flavonol, and flavanone aglycones by negative ion liquid chromatography electrospray ion trap mass spectrometry. *J. Am. Soc. Mass Spectrom.* **2001**, *12*, 707–715. [[CrossRef](#)]
65. Wang, Y.; Xu, Z.; Huang, Y.; Wen, X.; Wu, Y.; Zhao, Y.; Ni, Y. Extraction, purification, and hydrolysis behavior of apigenin-7-O-Glucoside from *Chrysanthemum Morifolium* tea. *Molecules* **2018**, *23*, 2933. [[CrossRef](#)] [[PubMed](#)]
66. Prasain, J.K.; Jones, K.; Kirk, M.; Wilson, L.; Smith-Johnson, M.; Weaver, C.; Barnes, S. Profiling and quantification of isoflavonoids in kudzu dietary supplements by high-performance liquid chromatography and electrospray ionization tandem mass spectrometry. *J. Agric. Food Chem.* **2003**, *51*, 4213–4218. [[CrossRef](#)] [[PubMed](#)]
67. Carvalho, A.A.; dos Santos, L.R.; de Freitas, J.S.; de Sousa, R.P.; de Farias, R.R.S.; Vieira Júnior, G.M.; Rai, M.; Chaves, M.H. First report of flavonoids from leaves of *Machaerium acutifolium* by DI-ESI-MS/MS. *Arab. J. Chem.* **2022**, *15*, 103765. [[CrossRef](#)]
68. Sayed, D.; Afifi, A.; Temraz, A.; Ahmed, A. Metabolic Profiling of *Mimusops elengi* Linn. Leaves extract and *in silico* anti-inflammatory assessment targeting NLRP3 inflammasome. *Arab. J. Chem.* **2023**, *16*, 104753. [[CrossRef](#)]
69. Tsugawa, H.; Cajka, T.; Kind, T.; Ma, Y.; Higgins, B.; Ikeda, K.; Kanazawa, M.; VanderGheynst, J.; Fiehn, O.; Arita, M. MS-DIAL: Data-independent MS/MS deconvolution for comprehensive metabolome analysis. *Nat. Methods* **2015**, *12*, 523–526. [[CrossRef](#)]
70. Shibabaw, A.; Abebe, T.; Mihret, A. Antimicrobial susceptibility pattern of nasal *Staphylococcus aureus* among Dessie Referral Hospital health care workers, Dessie, Northeast Ethiopia. *Int. J. Infect. Dis.* **2014**, *25*, 22–25. [[CrossRef](#)] [[PubMed](#)]
71. Alotaibi, B.; El-Masry, T.A.; Elekhawwy, E.; El-Kadem, A.H.; Saleh, A.; Negm, W.A.; Abdelkader, D.H. Aqueous core epigallocatechin gallate PLGA nanocapsules: Characterization, antibacterial activity against uropathogens, and *in vivo* reno-protective effect in cisplatin induced nephrotoxicity. *Drug Deliv.* **2022**, *29*, 1848–1862. [[CrossRef](#)]

72. Abbas, H.A.; Atallah, H.; El-Sayed, M.A.; El-Ganiny, A.M. Diclofenac mitigates virulence of multidrug-resistant *Staphylococcus aureus*. *Arch. Microbiol.* **2020**, *202*, 2751–2760. [[CrossRef](#)]
73. Binsuwaidan, R.; Sultan, A.A.; Negm, W.A.; Attallah, N.G.; Alqahtani, M.J.; Hussein, I.A.; Shaldam, M.A.; El-Sherbeni, S.A.; Elekhrawy, E. Bilosomes as nanoplatform for oral delivery and modulated *in vivo* antimicrobial activity of lycopene. *Pharmaceuticals* **2022**, *15*, 1043. [[CrossRef](#)]
74. Stepanović, S.; Vuković, D.; Hola, V.; Bonaventura, G.D.; Djukić, S.; Ćirković, I.; Ruzicka, F. Quantification of biofilm in microtiter plates: Overview of testing conditions and practical recommendations for assessment of biofilm production by staphylococci. *APMIS* **2007**, *115*, 891–899. [[CrossRef](#)]
75. Khayat, M.T.; Abbas, H.A.; Ibrahim, T.S.; Khayyat, A.N.; Alharbi, M.; Darwish, K.M.; Elhady, S.S.; Khafagy, E.-S.; Safo, M.K.; Hegazy, W.A. Anti-Quorum Sensing Activities of Gliptins against *Pseudomonas aeruginosa* and *Staphylococcus aureus*. *Biomedicines* **2022**, *10*, 1169. [[CrossRef](#)]
76. Schmittgen, T.D. *Real-Time Quantitative PCR*; Cold Spring Harbor Laboratory Press: Cold Spring Harbor, NY, USA, 2001.
77. Nejabatdoust, A.; Zamani, H.; Salehzadeh, A. Functionalization of ZnO nanoparticles by glutamic acid and conjugation with thiosemicarbazide alters expression of efflux pump genes in multiple drug-resistant *Staphylococcus aureus* strains. *Microb. Drug Resist.* **2019**, *25*, 966–974. [[CrossRef](#)] [[PubMed](#)]
78. Mastoor, S.; Nazim, F.; Rizwan-ul-Hasan, S.; Ahmed, K.; Khan, S.; Ali, S.N.; Abidi, S.H. Analysis of the antimicrobial and anti-biofilm activity of natural compounds and their analogues against *Staphylococcus aureus* isolates. *Molecules* **2022**, *27*, 6874. [[CrossRef](#)]
79. Zhang, S.; Qu, X.; Tang, H.; Wang, Y.; Yang, H.; Yuan, W.; Yue, B. Diclofenac Resensitizes Methicillin-Resistant *Staphylococcus aureus* to β -Lactams and Prevents Implant Infections. *Adv. Sci.* **2021**, *8*, 2100681. [[CrossRef](#)] [[PubMed](#)]
80. Stackhouse, R.R.; Faith, N.G.; Kaspar, C.W.; Czuprynski, C.J.; Wong, A.C.L. Survival and virulence of *Salmonella enterica* serovar enteritidis filaments induced by reduced water activity. *Appl. Environ. Microbiol.* **2012**, *78*, 2213–2220. [[CrossRef](#)]
81. Al-Kuraishy, H.M.; Al-Gareeb, A.I.; Albogami, S.M.; Jean-Marc, S.; Nadwa, E.H.; Hafiz, A.A.; A. Negm, W.; Kamal, M.; Al-Jouboury, M.; Elekhrawy, E.; et al. Potential Therapeutic Benefits of Metformin Alone and in Combination with Sitagliptin in the Management of Type 2 Diabetes Patients with COVID-19. *Pharmaceuticals* **2022**, *15*, 1361. [[CrossRef](#)]
82. Bancroft, J.D.; Gamble, M. *Theory and Practice of Histological Techniques*; Elsevier Health Sciences: Philadelphia, PA, USA, 2008.
83. Miotto, A.; Lins, T.A.; Montero, E.; Oshima, C.; Alonso, L.G.; Perfeito, J.A. Immunohistochemical analysis of the COX-2 marker in acute pulmonary injury in rats. *Ital. J. Anat. Embryol. Arch. Ital. Anat. Embriol.* **2009**, *114*, 193–199.
84. Anand, U.; Jacobo-Herrera, N.; Altemimi, A.; Lakhssassi, N. A comprehensive review on medicinal plants as antimicrobial therapeutics: Potential avenues of biocompatible drug discovery. *Metabolites* **2019**, *9*, 258. [[CrossRef](#)]
85. Miethke, M.; Pieroni, M.; Weber, T.; Brönstrup, M.; Hammann, P.; Halby, L.; Arimondo, P.B.; Glaser, P.; Aigle, B.; Bode, H.B. Towards the sustainable discovery and development of new antibiotics. *Nat. Rev. Chem.* **2021**, *5*, 726–749. [[CrossRef](#)]
86. Min, C.; Wang, H.; Xia, F.; Tang, M.; Li, J.; Hu, Y.; Dou, Q.; Zou, M. Characteristics of *Staphylococcus aureus* small colony variants isolated from wound specimen of a tertiary care hospital in China. *J. Clin. Lab. Anal.* **2022**, *36*, e24121. [[CrossRef](#)]
87. Sapkota, J.; Sharma, M.; Jha, B.; Bhatt, C.P. Prevalence of *Staphylococcus aureus* isolated from clinical samples in a tertiary care hospital: A descriptive cross-sectional study. *JNMA J. Nepal. Med. Assoc.* **2019**, *57*, 398. [[CrossRef](#)]
88. Idrees, M.M.; Saeed, K.; Shahid, M.A.; Akhtar, M.; Qammar, K.; Hassan, J.; Khaliq, T.; Saeed, A. Prevalence of *mecA*- and *mecC*-associated methicillin-resistant *Staphylococcus aureus* in clinical specimens, Punjab, Pakistan. *Biomedicines* **2023**, *11*, 878. [[CrossRef](#)]
89. Chew, C.H.; Yeo, C.C.; Che Hamzah, A.M.; Al-Trad, E.a.I.; Jones, S.U.; Chua, K.H.; Puah, S.M. Multidrug-Resistant Methicillin-Resistant *Staphylococcus aureus* Associated with Hospitalized Newborn Infants. *Diagnostics* **2023**, *13*, 1050. [[CrossRef](#)]
90. Steinig, E.J.; Duchene, S.; Robinson, D.A.; Monecke, S.; Yokoyama, M.; Laabei, M.; Slickers, P.; Andersson, P.; Williamson, D.; Kearns, A. Evolution and global transmission of a multidrug-resistant, community-associated methicillin-resistant *Staphylococcus aureus* lineage from the Indian subcontinent. *mBio* **2019**, *10*, 1–20. [[CrossRef](#)]
91. Raut, S.; Bajracharya, K.; Adhikari, J.; Pant, S.S.; Adhikari, B. Prevalence of methicillin resistant *Staphylococcus aureus* in Lumbini medical college and teaching hospital, Palpa, Western Nepal. *BMC Res. Notes* **2017**, *10*, 187. [[CrossRef](#)]
92. Muhaidat, R.; Al-Qudah, M.A.; Samir, O.; Jacob, J.H.; Hussein, E.; Al-Tarawneh, I.N.; Bsoul, E.; Orabi, S.T.A. Phytochemical investigation and *in vitro* antibacterial activity of essential oils from *Cleome droserifolia* (Forssk.) Delile and *C. trinervia* Fresen. (Cleomaceae). *S. Afr. J. Bot.* **2015**, *99*, 21–28. [[CrossRef](#)]
93. Tatsimo, S.J.N.; Tamokou, J.d.D.; Havyarimana, L.; Csupor, D.; Forgo, P.; Hohmann, J.; Kuate, J.-R.; Tane, P. Antimicrobial and antioxidant activity of kaempferol rhamnoside derivatives from *Bryophyllum pinnatum*. *BMC Res. Notes* **2012**, *5*, 158. [[CrossRef](#)]
94. Rho, H.S.; Ghimeray, A.K.; Yoo, D.S.; Ahn, S.M.; Kwon, S.S.; Lee, K.H.; Cho, D.H.; Cho, J.Y. Kaempferol and kaempferol rhamnosides with depigmenting and anti-inflammatory properties. *Molecules* **2011**, *16*, 3338–3344. [[CrossRef](#)]
95. Kalai, F.Z.; Boulaaba, M.; Ferdousi, F.; Isoda, H. Effects of isorhamnetin on diabetes and its associated complications: A review of *in vitro* and *in vivo* studies and a post hoc transcriptome analysis of involved molecular pathways. *Int. J. Mol. Sci.* **2022**, *23*, 704. [[CrossRef](#)] [[PubMed](#)]
96. Faleye, O.S.; Lee, J.-H.; Lee, J. Selected flavonoids exhibit antibiofilm and antibacterial effects against *Vibrio* by disrupting membrane integrity, virulence and metabolic activities. *Biofilm* **2023**, *6*, 100165. [[CrossRef](#)] [[PubMed](#)]

97. Wang, Y.; Chen, J.; Wang, Y.; Zheng, F.; Qu, M.; Huang, Z.; Yan, J.; Bao, F.; Li, X.; Sun, C. Cyanidin-3-O-glucoside extracted from the Chinese bayberry (*Myrica rubra* Sieb. et Zucc.) alleviates antibiotic-associated diarrhea by regulating gut microbiota and down-regulating inflammatory factors in NF- κ B pathway. *Front. Nutr.* **2022**, *9*, 970530. [[CrossRef](#)]
98. Frountzas, M.; Karanikli, E.; Toutouza, O.; Sotirakis, D.; Schizas, D.; Theofilis, P.; Tousoulis, D.; Toutouzas, K.G. Exploring the Impact of Cyanidin-3-Glucoside on Inflammatory Bowel Diseases: Investigating New Mechanisms for Emerging Interventions. *Int. J. Mol. Sci.* **2023**, *24*, 9399. [[CrossRef](#)]
99. Kalia, V.C.; Patel, S.K.; Lee, J.-K. Bacterial biofilm inhibitors: An overview. *Ecotoxicol. Environ. Saf.* **2023**, *264*, 115389. [[CrossRef](#)]
100. Sharma, D.; Misba, L.; Khan, A.U. Antibiotics versus biofilm: An emerging battleground in microbial communities. *Antimicrob. Resist. Infect. Control* **2019**, *8*, 76. [[CrossRef](#)]
101. Sedarat, Z.; Taylor-Robinson, A.W. Biofilm formation by pathogenic bacteria: Applying a *Staphylococcus aureus* model to appraise potential targets for therapeutic intervention. *Pathogens* **2022**, *11*, 388. [[CrossRef](#)]
102. Haddad, O.; Merghni, A.; Elargoubi, A.; Rhim, H.; Kadri, Y.; Mastouri, M. Comparative study of virulence factors among methicillin resistant *Staphylococcus aureus* clinical isolates. *BMC Infect. Dis.* **2018**, *18*, 560. [[CrossRef](#)]
103. Vlachou, M.; Karalis, V. An *in vitro*–*in vivo* simulation approach for the prediction of bioequivalence. *Materials* **2021**, *14*, 555. [[CrossRef](#)]
104. Hou, K.; Wu, Z.-X.; Chen, X.-Y.; Wang, J.-Q.; Zhang, D.; Xiao, C.; Zhu, D.; Koya, J.B.; Wei, L.; Li, J. Microbiota in health and diseases. *Signal Transduct. Target. Ther.* **2022**, *7*, 135. [[CrossRef](#)]
105. Jang, D.-i.; Lee, A.-H.; Shin, H.-Y.; Song, H.-R.; Park, J.-H.; Kang, T.-B.; Lee, S.-R.; Yang, S.-H. The role of tumor necrosis factor alpha (TNF- α) in autoimmune disease and current TNF- α inhibitors in therapeutics. *Int. J. Mol. Sci.* **2021**, *22*, 2719. [[CrossRef](#)] [[PubMed](#)]
106. Alomair, B.M.; Al-Kuraishy, H.M.; Al-Buhadily, A.K.; Al-Gareeb, A.I.; De Waard, M.; Elekhaway, E.; Batiha, G.E.-S. Is sitagliptin effective for SARS-CoV-2 infection: False or true prophecy? *Inflammopharmacology* **2022**, *30*, 2411–2415. [[CrossRef](#)] [[PubMed](#)]
107. Kaneko, N.; Kurata, M.; Yamamoto, T.; Morikawa, S.; Masumoto, J. The role of interleukin-1 in general pathology. *Inflamm. Regen.* **2019**, *39*, 12. [[CrossRef](#)] [[PubMed](#)]
108. Batiha, G.E.-S.; Al-Gareeb, A.I.; Elekhaway, E.; Al-Kuraishy, H.M. Potential role of lipoxin in the management of COVID-19: A narrative review. *Inflammopharmacology* **2022**, *30*, 1993–2001. [[CrossRef](#)] [[PubMed](#)]
109. Hirano, T. IL-6 in inflammation, autoimmunity and cancer. *Int. Immunol.* **2021**, *33*, 127–148. [[CrossRef](#)] [[PubMed](#)]
110. Nadwa, E.H.; Al-Kuraishy, H.M.; Al-Gareeb, A.I.; Elekhaway, E.; Albogami, S.M.; Alorabi, M.; Batiha, G.E.-S.; De Waard, M. Cholinergic dysfunction in COVID-19: Frantic search and hoping for the best. *Naunyn-Schmiedeberg's Arch. Pharmacol.* **2023**, *396*, 453–468. [[CrossRef](#)]
111. Al-Kuraishy, H.M.; Al-Gareeb, A.I.; Elekhaway, E.; Batiha, G.E.-S. Dipyridamole and adenosinergic pathway in COVID-19: A juice or holy grail. *Egypt. J. Med. Hum. Genet.* **2022**, *23*, 140. [[CrossRef](#)]

Disclaimer/Publisher's Note: The statements, opinions and data contained in all publications are solely those of the individual author(s) and contributor(s) and not of MDPI and/or the editor(s). MDPI and/or the editor(s) disclaim responsibility for any injury to people or property resulting from any ideas, methods, instructions or products referred to in the content.